

CERN-INTC-2005-021

INTC-P-197

April 2005

**Proposal to the INTC Committee**

# n\_TOF-Ph2

*The physics case and the related proposal for measurements at the CERN Neutron Time-of-Flight facility n\_TOF in the period 2006-2010*

*(The n\_TOF Phase-2 initiative)*

*Edited on behalf of the n\_TOF Collaboration Board by:*

A Mengoni (CERN, Geneva/ENEA, Bologna)

F Käppeler (FZK, Karlsruhe)

E Gonzales Romero (CIEMAT, Madrid)



U. Abbondanno<sup>20</sup>, H. Álvarez<sup>36</sup>, F. Alvarez-Velarde<sup>33</sup>, S. Andriamonje<sup>9</sup>, J. Andrzejewski<sup>28</sup>, P. Assimakopoulos<sup>12</sup>, L. Audouin<sup>11</sup>, G. Badurek<sup>1</sup>, P. Baumann<sup>8</sup>, F. Bečvář<sup>5</sup>, E. Berthoumieux<sup>9</sup>, A. Borella<sup>9</sup>, F. Calviño<sup>37</sup>, D. Cano-Ott<sup>33</sup>, R. Capote<sup>35,2</sup>, A. Carrillo de Albornoz<sup>30</sup>, P. Cennini<sup>39</sup>, V. Chepel<sup>29</sup>, N. Colonna<sup>19</sup>, G. Cortes<sup>37</sup>, A. Couture<sup>42</sup>, J. Cox<sup>42</sup>, S. David<sup>7</sup>, I. Dillmann<sup>11</sup>, C. Domingo-Pardo<sup>34</sup>, W. Dridi<sup>9</sup>, I. Duran<sup>36</sup>, M. Embid-Segura<sup>33</sup>, L. Ferrant<sup>7</sup>, A. Ferrari<sup>39</sup>, R. Ferreira-Marques<sup>29</sup>, K. Fujii<sup>20</sup>, W. Furman<sup>31</sup>, S. Ganesan<sup>16</sup>, C. Guerrero<sup>33</sup>, I. Goncalves<sup>30</sup>, R. Gallino<sup>23</sup>, E. Gonzalez-Romero<sup>33</sup>, A. Goverdovski<sup>32</sup>, F. Gramegna<sup>18</sup>, F. Gunsing<sup>9</sup>, R. Haight<sup>40</sup>, M. Heil<sup>11</sup>, A. Herrera-Martinez<sup>39</sup>, M. Igashira<sup>25</sup>, E. Jericha<sup>1</sup>, Y. Kadi<sup>39</sup>, F. Käppeler<sup>11</sup>, D. Karamanis<sup>12</sup>, D. Karadimos<sup>12</sup>, M. Kerveno<sup>8</sup>, V. Ketlerov<sup>32</sup>, G. Kim<sup>27</sup>, P. Koehler<sup>41</sup>, V. Konovalov<sup>31</sup>, E. Kossionides<sup>14</sup>, M. Krtička<sup>5</sup>, C. Lamboudis<sup>13</sup>, H. Leeb<sup>1</sup>, A. Lindote<sup>29</sup>, I. Lopes<sup>29</sup>, M. Lozano<sup>35</sup>, S. Lukic<sup>8</sup>, J. Marganiec<sup>28</sup>, L. Marques<sup>30</sup>, G. Martin Hernandez<sup>4</sup>, S. Marrone<sup>19</sup>, P. Mastinu<sup>18</sup>, A. Mengoni<sup>39,17</sup>, P.M. Milazzo<sup>20</sup>, C. Moreau<sup>20</sup>, M. Mosconi<sup>11</sup>, Y. Nagai<sup>26</sup>, F. Neves<sup>29</sup>, H. Oberhummer<sup>1</sup>, S. O'Brien<sup>42</sup>, M. Oshima<sup>24</sup>, J. Pancin<sup>9</sup>, C. Papachristodoulou<sup>12</sup>, C. Papadopoulos<sup>15</sup>, C. Paradela<sup>36</sup>, N. Patronis<sup>12</sup>, A. Pavlik<sup>1</sup>, P. Pavlopoulos<sup>10</sup>, R. Plag<sup>11</sup>, A. Plompen<sup>3</sup>, A. Poch<sup>37</sup>, C. Pretel<sup>37</sup>, J. Quesada<sup>35</sup>, T. Rauscher<sup>38</sup>, R. Reifarth<sup>40</sup>, C. Rubbia<sup>21</sup>, G. Rudolf<sup>8</sup>, P. Rullhusen<sup>3</sup>, J. Salgado<sup>30</sup>, C. Stephan<sup>7</sup>, G. Tagliente<sup>19</sup>, J.L. Tain<sup>34</sup>, L. Tassan-Got<sup>7</sup>, L. Tavora<sup>30</sup>, R. Terlizzi<sup>19</sup>, G. Vannini<sup>22</sup>, P. Vaz<sup>30</sup>, A. Ventura<sup>17</sup>, D. Villamarin<sup>33</sup>, M.C. Vincente<sup>33</sup>, V. Vlachoudis<sup>39</sup>, R. Vlastou<sup>15</sup>, F. Voss<sup>11</sup>, S. Walter<sup>11</sup>, M. Wiescher<sup>42</sup>

## The n\_TOF Collaboration

1. *Atominstytut der Österreichischen Universitäten, Technische Universität Wien, Austria*
2. *IAEA – Nuclear Data Section, Vienna, Austria*
3. *CEC-JRC-IRMM, Geel, Belgium*
4. *Centro de Aplicaciones Tecnológicas y Desarrollo Nuclear, Havana, Cuba*
5. *Charles University, Prague, Czech Republic*
6. *Centre National de la Recherche Scientifique/IN2P3 - CENBG, Bordeaux, France*
7. *Centre National de la Recherche Scientifique/IN2P3 - IPN, Orsay, France*
8. *Centre National de la Recherche Scientifique/IN2P3 - IReS, Strasbourg, France*
9. *CEA/Saclay - DSM, Gif-sur-Yvette, France*
10. *Pôle Universitaire Léonard de Vinci, Paris La Défense, France*
11. *Forschungszentrum Karlsruhe GmbH (FZK), Institut für Kernphysik, Germany*
12. *University of Ioannina, Greece*
13. *Aristotle University of Thessaloniki, Greece*
14. *NCSR, Athens, Greece*
15. *National Technical University of Athens, Greece*
16. *Bhabha Atomic Research Centre, Mumbai, India*
17. *ENEA, Bologna, Italy*
18. *Laboratori Nazionali di Legnaro, Italy*
19. *Istituto Nazionale di Fisica Nucleare, Bari, Italy*
20. *Istituto Nazionale di Fisica Nucleare, Trieste, Italy*
21. *Università degli Studi Pavia, Italy*
22. *Dipartimento di Fisica, Università di Bologna, and Sezione INFN di Bologna, Italy*
23. *Dipartimento di Fisica Generale, Università di Torino and Sezione INFN di Torino, Italy*
24. *Japan Atomic Energy Research Institute, Tokai-mura, Japan*
25. *Tokyo Institute of Technology, Tokyo, Japan*
26. *Osaka University, RCNP, Osaka, Japan*
27. *Kyungpook National University, Daegu, Korea*
28. *University of Lodz, Poland*
29. *LIP - Coimbra & Departamento de Fisica da Universidade de Coimbra, Portugal*

30. *Instituto Tecnológico e Nuclear, Lisbon, Portugal*
31. *Joint Institute for Nuclear Research, Frank Laboratory of Neutron Physics, Dubna, Russia*
32. *Institute of Physics and Power Engineering, Kaluga region, Obninsk, Russia*
33. *Centro de Investigaciones Energeticas Medioambientales y Technologicas, Madrid, Spain*
34. *Consejo Superior de Investigaciones Cientificas - University of Valencia, Spain*
35. *Universidad de Sevilla, Spain*
36. *Universidade de Santiago de Compostela, Spain*
37. *Universitat Politecnica de Catalunya, Barcelona, Spain,*
38. *Department of Physics and Astronomy - University of Basel, Switzerland*
39. *CERN, Geneva, Switzerland*
40. *Los Alamos National Laboratory, New Mexico, USA*
41. *Oak Ridge National Laboratory, Physics Division, Oak Ridge, USA*
42. *University of Notre Dame, Notre Dame, USA*

# Table of Contents

<b>ABSTRACT</b>	<b>7</b>
<b>SUMMARY TABLE OF THE PROPOSED MEASUREMENTS</b>	<b>9</b>
<b>INTRODUCTION</b>	<b>11</b>
<b>GENERAL MOTIVATIONS</b>	<b>13</b>
1. The physics case for neutron cross section measurements for nuclear astrophysics	13
2. The physics case for nuclear data measurements for advanced nuclear technologies and nuclear waste transmutation	16
3. The physics case for neutron cross section measurements for basic nuclear physics	20
<b>FACILITY</b>	<b>22</b>
Interventions in the present target-cooling assembly configuration	22
The Second n_TOF beam-line	22
The Second n_TOF experimental area (EAR-2)	24
<b>CAPTURE STUDIES</b>	<b>27</b>
Introduction	27
Nuclear Astrophysics	27
Stellar neutron capture cross sections of Mo, Ru, and Pd isotopes	27
The s-process efficiency in massive stars	28
Radioactive branch points and stellar neutron poisons	29
Nuclear waste transmutation & related nuclear technology studies	31
<b>NEUTRON INDUCED FISSION STUDIES</b>	<b>34</b>
Introduction	34
Measurement of the $^{235}\text{U}$ fission cross section up to 150 MeV	35
Fragment Distributions of Vibrational Resonances at the Fission Barrier	38

Fission cross sections and related measurements with PPACs detectors	40
Fission-fragments angular distributions	41
Fission-fragments yields	43
<b>OTHER REACTIONS</b>	<b>45</b>
(n,p), (n, $\alpha$ ), and (n,xc) reactions	45
Detection systems 1: Compensated Ion Chamber (CIC)	47
Detection systems 2: MICROMEGAS	48
Detection systems 3: $\Delta E$ -E telescopes	49
Neutron scattering reactions	50
<b>MEASUREMENTS RELATED TO DETECTOR DEVELOPMENTS</b>	<b>53</b>
Gas detectors	53
Neutron cross-section measurements of relevance for Radiation Dosimetry, Radiation Protection and Radiation Transport	54
<b>REFERENCES</b>	<b>57</b>

## **ABSTRACT**

The following document represents a proposal for the experimental program to be performed at the CERN Neutron Time-of-Flight facility n\_TOF for the period 2006-2010. The experimental program follows the lines defined during the first three experimental campaigns in 2002, 2003, and 2004, which identified the three main objectives of the experimental activities at n\_TOF: (1) neutron cross section measurements for nuclear astrophysics, (2) nuclear data measurements for advanced nuclear technologies and nuclear waste transmutation, and (3) neutron cross section measurements for basic nuclear physics.

After a description of the physics case for the three main lines of activity, the experimental plan for each group of measurements is outlined in some detail. The most important measurements to be performed during the second phase of activities (n\_TOF-Ph2) are identified and the related detection systems are described.

A first sketch of the proposal for the construction of a second neutron beam line and of the corresponding experimental area (EAR-2) is presented together with a discussion of the decisive improvements, which this initiative would bring in terms of neutron intensity, background conditions, and a more efficient use of the facility.





## SUMMARY TABLE OF THE PROPOSED MEASUREMENTS

This summary table contains a list of the proposed measurements for the n\_TOF-Ph2 period (2006-2010). Measurements which require the second beam line and its related experimental area (**EAR-2**) are marked in **red**.

Capture measurements	
Mo, Ru, Pd stable isotopes	calculation of r-process residuals isotopic patterns in SiC grains
Fe, Ni, Zn, Se stable isotopes	s-process nucleosynthesis in massive stars accurate nuclear data needs for structural materials
A $\approx$ 150 (isotopes varii)	s-process branching points long-lived fission products
<sup>234,236</sup> U, <sup>231,233</sup> Pa	Th/U nuclear fuel cycle
<sup>235,238</sup> U	standards, conventional U/Pu fuel cycle
<sup>239,240,242</sup> Pu, <sup>241,243</sup> Am, <sup>245</sup> Cm	incineration of minor actinides
<sup>197</sup> Au, C, Pb	Calibrations
Fission measurements	
<sup>231</sup> Pa, <sup>245</sup> Cm, <sup>241</sup> Pu, <sup>241,243</sup> Am, <sup>244</sup> Cm	fission cross section data for minor actinides
<sup>235</sup> U(n,f) with p(n,p')	new <sup>235</sup> U(n,f) cross section standard
Varii	FF angular distribution
Varii	FF mass distribution
<sup>234</sup> U(n,f)	study of vibrational resonances at the fission barrier
Other measurements	
<sup>147</sup> Sm(n, $\alpha$ ), <sup>67</sup> Zn(n, $\alpha$ ), <sup>99</sup> Ru(n, $\alpha$ )	p-process studies
<sup>58</sup> Ni(n,p), other (n,lcp)	gas production in structural materials
Al, V, Cr, Zr, Th, <sup>238</sup> U(n,lcp)	structural and fuel material for ADS and other advanced nuclear reactors
He, Ne, Ar, Xe	low-energy nuclear recoils (development of gas detectors)
n+D <sub>2</sub>	neutron-neutron scattering length
Total reaction cross sections on various materials (C, N, O, etc.), CR-39 and TLD dosimetry	radiation protection, dosimetry and radiation transport



## INTRODUCTION

The experimental program at the CERN neutron Time-of-Flight facility n\_TOF in the three experimental campaigns in **2002, 2003 and 2004** has covered capture and fission cross section measurements on a large number of samples.

<b>Capture and Fission measurements</b>	
Measurements of capture and fission cross sections performed at CERN n_TOF during the <b>2002, 2003 and 2004</b> experimental campaigns. Radioactive species are marked in <b>bold</b> .	
<b>Capture measurements</b>	<b>Fission measurements</b>
<sup>151</sup> <b>Sm</b> <sup>204,206,207,208</sup> Pb <sup>209</sup> Bi <sup>232</sup> <b>Th</b> <sup>139</sup> La <sup>24,25,26</sup> Mg <sup>90,91,92,93,94,96</sup> Zr <sup>186,187,188</sup> Os <sup>233,234</sup> U <sup>237</sup> <b>Np</b> <sup>243</sup> <b>Am</b> <sup>240</sup> <b>Pu</b>	<sup>233,234,236</sup> U <sup>232</sup> <b>Th</b> <sup>237</sup> <b>Np</b> <sup>241,243</sup> <b>Am</b> <sup>245</sup> <b>Cm</b>
<sup>197</sup> Au	<sup>235,238</sup> U

Most of the measurements have been performed within the framework defined by the n\_TOF-ND-ADS Project (n\_TOF Nuclear Data for Accelerator Driven Systems), an FP5 initiative of the European Commission on basic studies for the Partitioning and Transmutation (P&T) of nuclear wastes. The motivations and physics cases of the various measurements have been provided in great detail in the proposals for measurements submitted to the CERN INTC Committee during the period 2000-2004 (n\_TOF-02 to n\_TOF-10). Most of the measurements had a strong relevance, unique in a few cases, in nuclear astrophysics, in particular for studies on s-process nucleosynthesis.

In the present proposal, the physics cases for measurements at n\_TOF for a “second phase” of activities (hence the title “n\_TOF-Ph2”) are discussed. The planned measurements are presented in sufficient detail for judging the relevance of the physics to be performed during the future operation of n\_TOF, presumably covering the period **2006-2010**.

After a general description of the physics cases for the three major lines of activities, Nuclear Astrophysics, Advanced Nuclear Technologies, and Basic Nuclear Physics, the proposals for different measurements, capture, fission and cross sections for some other reaction channels will be presented.

Of particular relevance in the present proposal is the plan for the construction of a **second beam line** and its related experimental area at a short distance from the spallation module (n\_TOF **EAR-2**). This additional beam line, approximately 20 m long, would allow for a new class of measurements at n\_TOF, enhancing further the unique characteristics of n\_TOF, in particular for the extremely high instantaneous flux obtainable (a factor of  $\sim 100$  higher than presently available in EAR-1 at a flight path of 185 m). The  $90^\circ$  angle between the incident proton beam and the new neutron beam line would, in addition, improve drastically the background conditions in particular those due to the high-energy particles at short times (“flash”). The opportunities for new classes of measurements at this proposed new beam line are underlined in the various proposals for measurements of capture, fission and other reaction channels.

An important aspect, which we want to stress in the Introduction, is the predicted availability of **protons** for n\_TOF. The facility is using the 20 GeV proton beam from the PS. A recent study of the CERN AB Department [1] showed that, giving the highest priorities to the LHC filling and the SPS experiments, approximately  $1.5 \times 10^{19}$  **protons** per year could be allocated to n\_TOF during the period 2006-2010, without any influence on other fixed target experiments. Considering that during the 2002-2004 period of operation the number of protons delivered to the n\_TOF target has been of the order of  $1.3 \times 10^{19}$  per year, it can be inferred that experimental campaigns similar to those successfully performed during the first three years of operation of n\_TOF could also be planned for the period 2006-2010. Hence, the present proposal has been well balanced in terms of proposed measurements along the three main lines of activities in Nuclear Astrophysics, Nuclear Technologies and Basic Nuclear Physics.

Finally, concerning the organizational aspects of the activities to be carried on during n\_TOF-Ph2, it is important to notice that a **Letter of Intent** has been signed by 24 research institutes (with a total of 42 research teams), comprising essentially all the partners in the previous n\_TOF Collaboration (listed in the n\_TOF Memorandum of Understanding for the period 2000-2004) as well as four Institutes from India, Cuba, China and South Korea. This Letter of Intent expresses the interest in the continuation of the n\_TOF activities and sets the basis for the construction of the new n\_TOF Memorandum of Understanding for n\_TOF-Ph2. It is foreseen to start the negotiation for a new MoU for the Phase-2, after the present scientific proposal has been endorsed by the INTC and approved by the CERN Research Board, hopefully within the end of 2005/beginning of 2006.

## GENERAL MOTIVATIONS

### 1. The physics case for neutron cross section measurements for nuclear astrophysics

All the elements heavier than iron are synthesized by neutron induced reactions. In particular, approximately half of the elemental abundances between iron and bismuth are produced by the slow neutron capture process (“*s* process”) while the other half is contributed by the rapid neutron capture process (“*r* process”). In this context, “rapid” or “slow” has to be associated with the rate of  $\beta$ -decay in comparison to the neutron capture rate<sup>1</sup>. Generally speaking, the *s* process can be associated with the quiet, slow burning phases of stellar evolution while the *r* process can be assigned to explosive scenarios such as supernovae.

Both, the *s* and *r* process are based on neutron capture reactions. In particular, for the *s* process, there is a direct correlation between the neutron capture cross section,  $\sigma(n,\gamma)$ , and the observed abundance of a given isotope in the universe. This correlation makes it necessary to measure the neutron capture cross sections of all isotopes along the valley of  $\beta$ -stability, a program which has been going on since the early days of nuclear astrophysics.

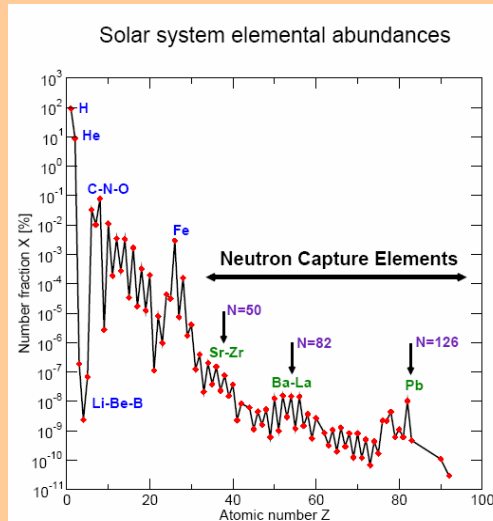
Recently, the simple picture just described has been enriched by the enormous progress made by astronomical observations of stellar spectra as well as by important developments in understanding and modeling stellar evolution. In the specific case of the *s* process, the present scenario is connected to the evolution of AGB (“Asymptotic Giant Branch”) stars. Moreover, the picture is

#### The *s* process

Neutrons can be produced during burning phases of stellar evolution by reactions such as  $^{13}\text{C}(\alpha,n)$  or  $^{22}\text{Ne}(\alpha,n)$ . When enough amount of seed material is available together with a sufficient neutron fluence, successive neutron captures on seed nuclei and  $\beta$ -decays along the stability valley lead to the synthesis of heavy elements. In the specific case of the *s* process, the seed material is  $^{56}\text{Fe}$ , which is the final product of charged-particle fusion reactions taking place in stars. A quantitative theory of the *s* process formulated by D. Clayton in the '60ies leads to the *s*-process condition

$$\langle\sigma_A\rangle\cdot N_A \approx \text{const.}$$

where  $\langle\sigma\rangle$  is the Maxwellian averaged neutron capture cross section and  $N$  is the abundance of the isotope with mass number  $A$ . From this relation it follows immediately that the abundances of nuclei with small neutron capture cross sections are enhanced. In fact, this is precisely what is observed in the solar-system abundance pattern.



<sup>1</sup> The half-life for  $\beta$ -decay is simply related to the beta decay rate  $\lambda_\beta$  by  $\tau_\beta = \ln 2 / \lambda_\beta$  while the neutron capture rate is  $\lambda_n = n \langle\sigma v\rangle$ . Here,  $n$  is neutron density,  $\sigma$  the neutron capture cross section and  $v$  the neutron velocity.

clear enough to disentangle the two  $s$  process components, responsible for the nucleosynthesis in two different stellar mass regimes: while the helium layers of thermally pulsing low mass AGB stars are efficiently producing the  $s$ -process abundances in the mass region  $90 < A < 209$ , massive stars contribute mostly to the region from  $A < 90$  down to iron. In any case neutron capture cross sections with accuracies at the level of a few percent are required for the quantitative description of  $s$ -process nucleosynthesis.

Not only the need for neutron capture cross sections is enhanced by these recent developments, but the necessity of *high accuracy* is evident. The accuracy at the level of a few percent is mandatory for studying the details of the process taking place in AGB stars in a realistic fashion.

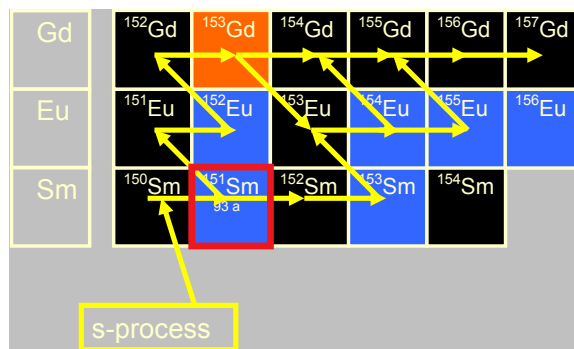


**Figure 1:**  $s$  process branchings in the mass region  $A \approx 150$ .

Particularly unique features of  $s$  process nucleosynthesis are branchings in the reaction path. Since typical neutron capture times are of the order of one year, the majority of unstable isotopes encountered by the neutron capture chain decays so fast that neutron capture becomes negligible. A number of isotopes, however, exhibit half lives comparable with the neutron capture time. The resulting competition gives rise to a branching of the reaction path, a local phenomenon that involves usually not more than eight isotopes before the branching is closed and the capture path continues as a single reaction chain.

Detailed analyses of such branchings are so fascinating because the evolving abundance patterns reflect the physical conditions at the stellar site of the  $s$  process. In the simplest case, this is the stellar neutron flux but there are branchings that are strongly determined by temperature, pressure or even by the convective motions in the deep stellar interior. Obviously, this type of information represents stringent tests for stellar models of the AGB phase, which is known to be the stage when the  $s$  process operates. A prominent example of a branching point is  $^{151}\text{Sm}$  sketched in Figure 1, which determines the reaction flow towards the  $s$ -only isotope  $^{152}\text{Gd}$ .

An essential piece of information for analysing the branchings in the reaction path are the neutron capture cross sections of the unstable branch point isotopes themselves. Such measurements are difficult because the radioactivity of the sample may cause excessive backgrounds in the detectors or may be unacceptable because of standard safety limits. Both problems suggest that sufficiently sensitive techniques are required, which can tolerate the use of extremely small samples.

From the detector side, the n\_TOF TAC, which has been built by the n\_TOF collaboration, represents an optimal solution due to the combination of high detection efficiency and excellent discrimination of  $\gamma$ -ray background. In addition to the optimized capture detector, the characteristics of the neutron source are of crucial importance. The neutron source is required to exhibit the highest possible flux in the energy range from 1 keV to 300 keV in order to compensate for the small sample mass. This clearly calls for a spallation neutron source. Another important requirement is that the source should operate at the lowest possible duty factor in order to obtain an efficient discrimination of the constant background from the sample activity via time-of-flight.

In its present design, the n\_TOF facility is already superior to other spallation sources thanks to the very high instantaneous flux, the low duty factor (repetition rate of the proton driver of only  $\approx 1$  Hz) and the short pulse width of 7 ns. While this geometry is perfect for high resolution measurements as well as for obtaining high fluxes at the highest possible neutron energies, an additional short flight path perpendicular to the proton beam would result in a unique neutron source for astrophysics applications as well as for measurements of relevance for transmutation. With such a short flight path the experimental sensitivity would be unique worldwide, thus allowing astrophysics measurements even on the very small unstable samples that could be produced on site at ISOLDE.

Another important astrophysical aspect concerns the origin of the 35 rare nuclei on the proton-rich side of the stability valley, which cannot be produced in either the *s*- or the *r*-process. Current scenarios are the hot, late phases in the evolution of massive stars, where sufficiently high temperatures are reached to produce these so-called *p* nuclei by photodisintegration. Although models of massive stars can reproduce the *p*-abundances across a range of nuclear masses, the regions  $A < 124$  and  $150 \leq A \leq 165$  remain problematic, either due to problems in the astrophysical models or due to severe uncertainties in the nuclear physics input. It has been found that the  $\alpha$ -nucleus optical potential needed for calculating the important stellar  $(\gamma, \alpha)$  and  $(n, \alpha)$  reaction rates is badly constrained at the low energies involved. The study of  $(n, \alpha)$  reactions at the n\_TOF facility will help to improve the optical potential and the respective nuclear reaction models significantly, an essential contribution for solving this persistent *p*-process puzzle.

### Asymptotic Giant Branch (AGB) stars

The large majority of all stars in the Universe that have left the quiescent central hydrogen burning phase, i.e., the main sequence, will reach their final evolutionary stage as stars on the asymptotic giant branch (AGB). This will also happen to our own Sun in about 8 billion years from now. An AGB-star is a cool, luminous, and unstable red giant star. It will gradually develop an intense wind that removes material from the surface at an increasing rate as the end is approached. This will have a profound effect on the evolution of the star, and it will eventually terminate its life as a star. Furthermore, the wind also carries the results of internal nuclear processes, activated during the AGB evolution, and hence contributes to the chemical evolution of the galaxies.

There is direct evidence for the *s*-process occurring in AGB stars: Technetium, with  $Z=43$  is an *s*-process element which is radioactive and has a half-life of only 200,000 years. It has been detected in AGB stars that are much older than that, thus demonstrating the occurrence of the *s*-process in such type of stars.

The *s*-process is taking place in a thin layer between the He and the H shells surrounding the C/O rich core of the AGB star. The *s*-process products are then brought to the stellar surface by recurrent episodes of deep mixing and they are carried into the interstellar medium by the strong stellar winds.

## 2. The physics case for nuclear data measurements for advanced nuclear technologies and nuclear waste transmutation

Nuclear waste is one of the main problems for the public acceptance of nuclear energy production and for the sustainability of this energy source. Although a deep underground repository seems to be a scientifically proven and technologically viable solution for the nuclear waste for the first thousands of years, this option presents difficulties for social acceptability. For this reason, nuclear waste transmutation has been proposed as a way to reduce the inventory of the long lived component of the nuclear waste – and mainly the trans-uranium actinides - by a factor of 100 or more.

Actinide transmutation is proposed to take place by fission in nuclear systems like critical reactors or subcritical accelerator driven systems (ADS). In most transmutation scenarios, the use of fast neutron energy spectra and specific fuel compositions, highly enriched in high mass trans-uranium actinides, are proposed. In addition, the transmutation of long-lived fission fragments has also been proposed using neutron absorption (mainly by radiative capture) normally in thermal and epithermal neutron energy spectra.

The present knowledge of the neutron cross sections of actinides is mainly related to the exploitation of the U-Pu cycle in nuclear reactors with a thermal neutron spectrum and to the design and operation of experimental fast U-Pu nuclear reactors. In addition, the currently existing nuclear data bases can be used for the conceptual design of the transmutation oriented nuclear devices – critical reactors or ADS – and for the first order evaluation of the impact of the transmutation technology in the nuclear waste management. However, the detailed **engineering designs, safety evaluations**, and the ultimate **performance assessment** of dedicated transmutation ADS and critical reactors (i.e. with fuels highly enriched in transuranic isotopes) require more **precise and complete basic nuclear data**. In addition, more accurate cross sections of the U-Pu fuel cycle isotopes, transuranic elements, and specific structural materials help to improve the safety and optimisation of present and future nuclear reactors.

The large amount of  $^{238}\text{U}$  in the current fuels, more than 95%, is the basis of the production of the highly radiotoxic actinides by successive neutron captures and beta decays, leading to the formation of isotopes of Pu, Am and Cm. Very accurate capture data are needed and for this reason an overwhelming quantity of neutron capture experiments on  $^{238}\text{U}$  exists and has formed the basis for the establishment of a secondary capture standard, which will be updated in the near future. New data on  $^{238}\text{U}(n,\gamma)$ , especially in a large energy range, are welcome to improve the precision of this standard. Since at nearly every time-of-flight facility a  $^{238}\text{U}$  capture experiment has been performed it is highly desirable to have such a data set for the n\_TOF facility with a high purity  $^{238}\text{U}$  sample (containing less than 100 ppm  $^{235}\text{U}$ ). In addition, these data will be considerably helpful in the analysis and interpretation of the measurements of the other actinides. An additional important quantity in current reactors is the capture to fission ratio of  $^{235}\text{U}$ . Although the fission cross section is considered a standard, the capture cross section is not, because of the difficulty of measuring the capture cross section of a fissile isotope. With the proposed capture setup at n\_TOF, including a fission veto detector, an accurate measurement of the  $^{235}\text{U}$  capture cross section comes within reach.



A different approach is to reduce the amount of nuclear waste, notably the higher actinides, by using a fuel cycle based on  $^{232}\text{Th}$ . The isotope  $^{232}\text{Th}$  itself is not fissile but after neutron capture followed by  $\beta$ -decay, the fissile isotope  $^{233}\text{U}$  is formed. The build-up of the higher actinides, especially americium and curium, is strongly suppressed due to the lower atomic and mass number of thorium. The use of the thorium cycle needs accurate data for isotopes that are less important in the conventional uranium cycle, and in particular capture data on  $^{232}\text{Th}$ ,  $^{233,234,236}\text{U}$  and  $^{231,233}\text{Pa}$ . The large radioactivity of  $^{231}\text{Pa}$  and the related safety issues has prevented a capture measurement in the first phase of n\_TOF. However, at the 20 m station (EAR-2), much lower sample masses are needed and therefore a low resolution capture measurement becomes possible. With a suitable sample, even the capture cross section of  $^{233}\text{Pa}$ , with a half life of only 27 days, can be measured with a sample of only several micrograms. The capture chain in the actinide region is shown in Figure 2.

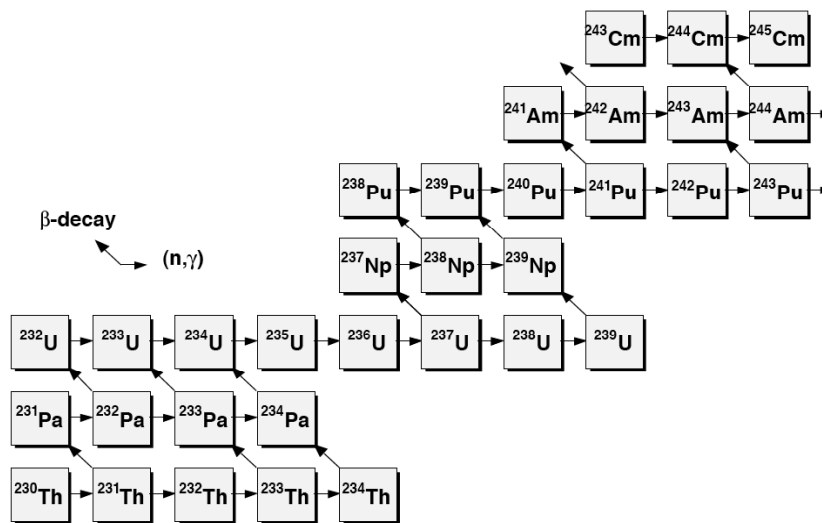


**Figure 2:** The relevant isotopes of the neutron capture and beta decay chain in the actinide region.

Of crucial importance is the composition of the fuels proposed for transmutation devices with a large concentration of minor actinides and higher plutonium isotopes. These isotopes with moderate relevance for the operation of present reactors will play an important role in the neutron balance of the transmuters.

The respective fuel compositions modify severely the role of the different isotopes for the global operation of the reactor and, in particular, for its transmutation performance. Figure 3 shows the relative contribution to the total number of captures from the different isotopes in the fuels previously described. Particular key isotopes for the transmutation scenarios, which are showing significant capture fractions, are  $^{237}\text{Np}$ ,  $^{238,239,240,241,242}\text{Pu}$ ,  $^{241,243}\text{Am}$  and  $^{244,245,246}\text{Cm}$ .

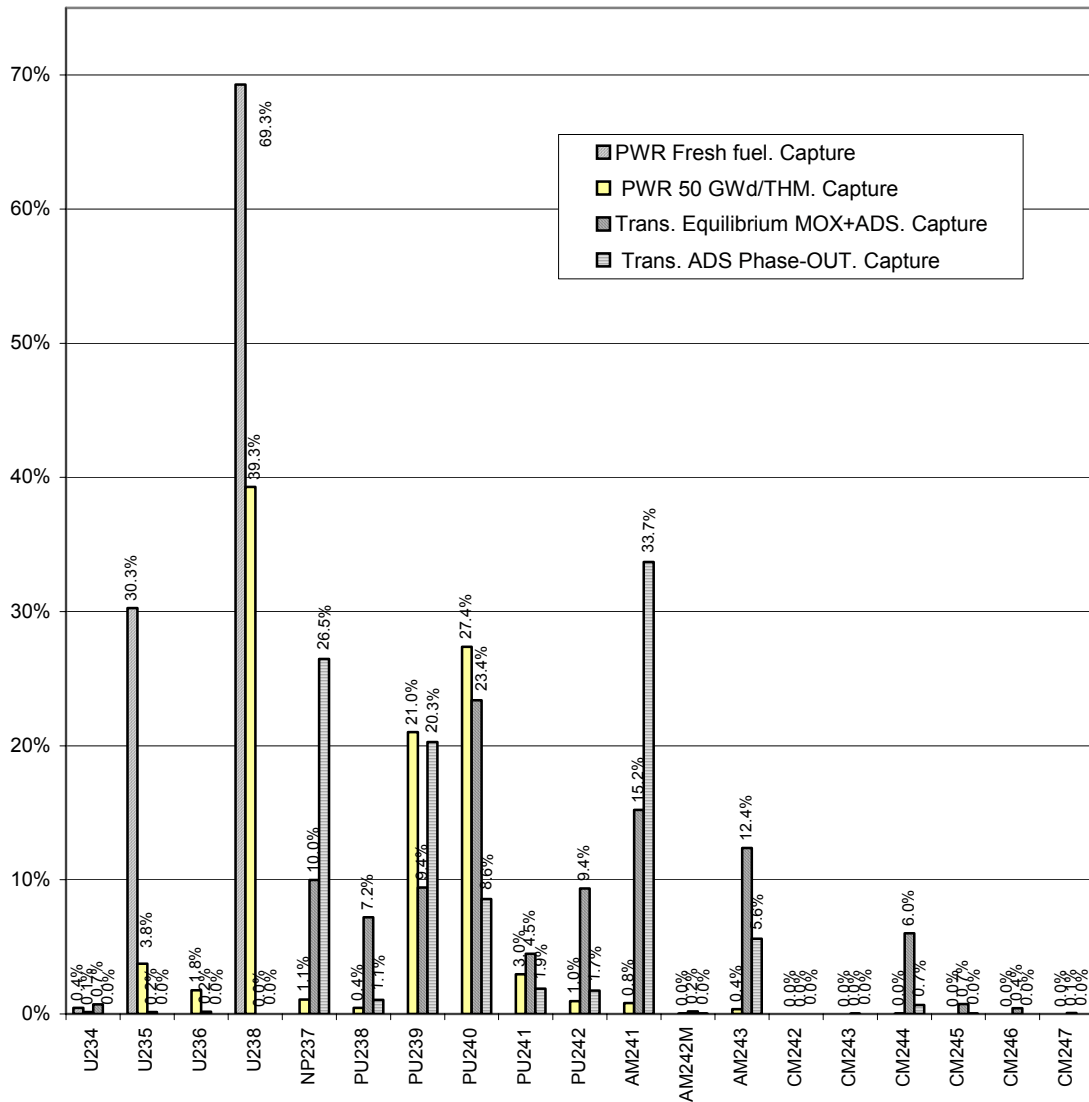


**Figure 3:** Capture contributions from the isotopes present in the fuels of different nuclear plants: PWR (fresh and irradiated fuels) and for two transmutation devices.

The high radioactivity and spontaneous fission probability of  $^{238}\text{Pu}$  ( $t_{1/2} = 87.74$  yr) and  $^{244}\text{Cm}$  ( $t_{1/2} = 18.1$  yr) makes it extremely difficult to perform the capture measurements of these isotopes at the present n\_TOF beam line. A new shorter beam line with higher instantaneous flux could make these measurements viable. In this case it could also be interesting to measure the neutron capture cross section of  $^{242\text{m}}\text{Am}$  ( $t_{1/2} = 141$  yr), the only long-lived even americium isotope.

Already in its present configuration, the n\_TOF facility offers worldwide unique features for performing the capture measurements discussed herein: it combines a high instantaneous neutron intensity at a very long flight path of 185 m, excellent energy resolution, a high-performance data acquisition system based on flash ADCs and a segmented BaF<sub>2</sub> total absorption calorimeter (TAC). As a remarkable example, at n\_TOF it has been possible to obtain the first direct neutron

capture cross section data in the resolved resonance region for the highly radioactive sample  $^{243}\text{Am}$ .

For these reasons, it is proposed to continue the experimental program on neutron capture cross section measurements for isotopes relevant to nuclear technology that was started successfully in 2004 as a part of the n\_TOF project.

### 3. The physics case for neutron cross section measurements for basic nuclear physics

A number of basic nuclear properties are commonly used in model calculations for neutron capture cross sections as well as for fission cross sections. One can think of nuclear masses, decay half-lives, level densities at high excitation energies, excitation strengths of giant resonances, fission barriers, and many others. Nuclear theories, both for nuclear structure as well as for reaction processes are normally developed on the basis of experimental knowledge. Hence, microscopic as well as phenomenological approaches are deeply dependent on data obtained in a continuing experimental effort.

A huge amount of experimental information is presently available for the development of nuclear structure and reaction models. However, most recently, a great effort has been devoted to expand the present knowledge in isospin space by studying nuclei far from the valley of  $\beta$ -stability. Only recently, with the availability of radioactive ion beams (RIBs), some of the nuclei far from stability in the low mass region have been accessed experimentally. However, for applications such as the physics of the  $r$  process, these nuclear properties need to be predicted by theoretical models.

Critical improvements on the reliability of theoretical model predictions could be reached by experiments dedicated to the accurate measurements of quantities such as **neutron strength functions, nuclear level densities, and reaction cross sections**. Especially at neutron shell closures, neutron strength functions and level densities are still not well known and also hard to predict. Experiments at n\_TOF can be used to determine such quantities. Likewise, a high energy resolution is useful to study the interplay between compound and direct capture mechanisms, which is important in nuclei with low level densities. Measurements focused on this point on closed-shell nuclei and/or on light nuclei will provide very useful information on nuclear structure and reaction mechanisms.

Along this line, one can observe that recent experiments with RIBs have shown the possibility of investigating reaction mechanisms as well as nuclear structure properties of unstable nuclei with reactions such as the **Coulomb dissociation** technique (Coulomb breakup). This process can be viewed as the **time-reversal invariant of the capture process**. In particular, the Coulomb dissociation into the  ${}^A_Z + n$  channel is the time-reversal of the neutron capture process. It is therefore evident that the possibility of performing neutron capture cross section measurements on unstable targets can provide crucial information on the possibility of applying the Coulomb dissociation techniques in experiments with RIBs, in addition to the direct determination of neutron capture rates on unstable nuclei. Meanwhile, the development of accurate models for the representation of the two basic reaction mechanisms, the direct and resonance processes, would allow to improve the reliability of such models in the extrapolation to nuclei far from the stability.

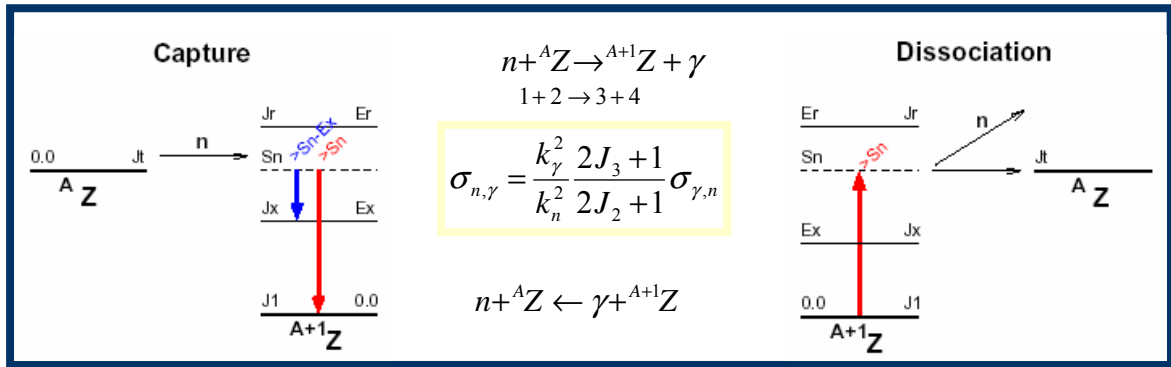


**Figure 4:** The neutron capture process and its time-reversal invariant, the photon (or Coulomb) dissociation.

The possibility of performing measurements on very small samples of a few micrograms will open completely new opportunities at n\_TOF. In fact, **in a combined effort with ISOLDE** a plan for measurements on radioactive samples, even with relatively short half-life would allow to study nuclear structure properties of unstable nuclei. Neutron capture  $\gamma$ -ray spectroscopy studies on stable isotopes have been one of the key tools for studying nuclear structure properties on stable nuclei and could in this way be expanded into the region of unstable species.

## FACILITY

As an introduction to this section it is to be emphasized – as it was said before - that the n\_TOF facility in its present form constitutes the most attractive neutron source for time-of-flight experiments worldwide. The options discussed here aim at substantial further improvements, which will allow a more flexible use of the facility and will greatly expand the experimental possibilities.

### Interventions in the present target-cooling assembly configuration

The use of H<sub>2</sub>O as the coolant for the n\_TOF target had severely hampered a number of measurements of (n,γ) cross section during the first phase of n\_TOF, because of a strong γ-ray background due to neutron captures in the hydrogen of the cooling water. These γ-rays are traveling along with the beam and are reaching the 185 m station EAR-1 together with neutrons in the energy range from a few keV up to several hundred keV. These γ-rays are scattered by the capture sample and cause a background in the C<sub>6</sub>D<sub>6</sub> detectors required for measurements of small, resonance-dominated capture cross sections, e.g. those of the important neutron magic isotopes. In fact, this background limits the sensitivity of the entire facility.

This background can be eliminated or substantially reduced either by adding boric acid to the cooling water or by replacing it with heavy water. The first option would provide a reduction by an order of magnitude and would also soften the spectrum of the in-beam γ-ray background considerably, while there are open problems with the filters in the coolant circuit. On the other hand, replacing the cooling water by D<sub>2</sub>O would reduce the intensity of the in-beam γ-rays by a factor of 100, thus practically eliminating the problem completely. In addition, this solution would also boost the neutron flux at keV energies by a factor of five.

The collaboration is, therefore, determined to implement the necessary modifications to the present n\_TOF target/moderation assembly configuration before the next measuring campaign in 2006, preferentially using the D<sub>2</sub>O option. In which way the necessary improvement can be achieved, are presently under discussion but will depend on the result of the technical inspection of the target planned for the summer of 2005.

### The Second n\_TOF beam-line

The long flight path of the present n\_TOF facility is of great advantage for measurements with high resolution in neutron energy. The overall efficiency of the experimental program and the range of possible measurements could be **enormously improved**, however, with the installation of an additional shorter flight path of approximately 20 m. There are two main reasons for this improvement

The existing flight path exhibits an angle of only 10 degrees with respect to the incident proton beam line. Therefore, a burst of weakly interacting relativistic

spallation products is emitted into the neutron flight path at each proton pulse. In spite of massive shieldings and the use of a sweeping magnet for deflecting the charged particles, a remaining background in form of a “**time-zero flash**” is causing an overload of the detectors and hampers measurements at high neutron energies. In particular, capture measurements with the total absorption BaF<sub>2</sub> calorimeter, fission studies with ionization chambers, and measurements with Ge detectors, e.g. of (n,xn) cross sections are strongly affected by this flash. Since all particles causing the flash are emitted in forward direction the flash would be **strongly reduced** at an angle of 90 degrees with respect to the proton beam direction.

The idea for an additional second beam line as sketched Figure 5 is making use of the existing vertical shaft, through which the spallation target was brought into its present position. Therefore, it would be sufficient to drill a narrow hole only a few cm in diameter from the surface to the service gallery above the target, not requiring an intervention in the critical zone around the target area itself.

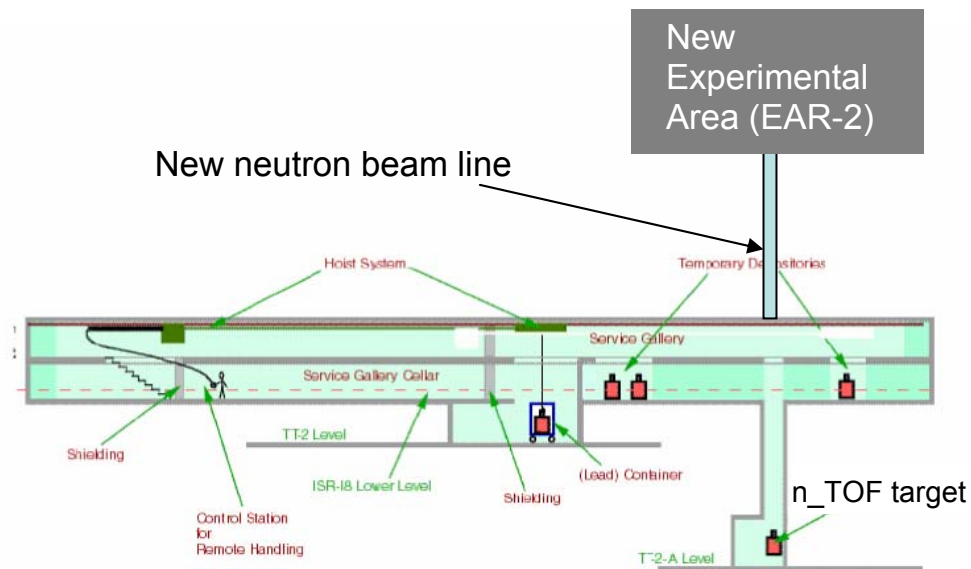


**Figure 5:** Layout of the second beam-line at approximately 20m from the spallation module.

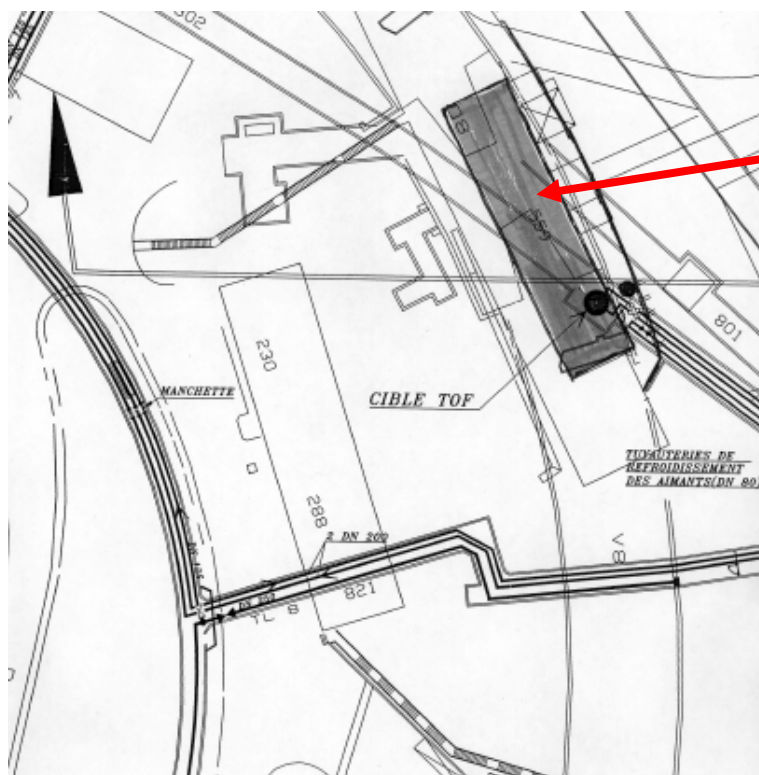
The second main motivation for the implementation of a second beam line is related to the possibility of obtaining a much **higher neutron flux** (a factor of roughly 100) with respect to the present neutron fluence in EAR-1 set at 185 m from the spallation module. This will be described in the following section.

## The Second n\_TOF experimental area (EAR-2)

The optimal condition for performing measurements on radioactive samples would be to have an experimental area as a Class-A laboratory. In this sort of laboratory, open radioactive sources can be handled and, therefore, used for measurements in a more flexible way. A non-exhaustive list of requirements for the EAR-2 are:

- Controlled Access
- Solid building, fire resistant for a certain time
- Monitored and filtered ventilation, guaranteeing an under pressure in the laboratories
- Wardrobe facilities to don special clothing
- Showers
- Monitoring: dose rate, aerosol concentration, hand-foot-monitor, portable monitors

The possible location of the EAR-2 with the vertical beam line is shown in the Figure 6 below. As can be seen, this is at present a part of building 559 (barrack) which could be rearranged in order to host the EAR-2 together with some offices.



Offices in  
Barrack 559

**Figure 6:** Vertical position of the n\_TOF target (“CIBLE TOF”) and the present location of the barrack 559.



The gain in experimental sensitivity that can be obtained in such an EAR-2 is best illustrated at the example of the capture data taken in 2002 with a sample containing 150 mg of  $^{151}\text{Sm}$ .

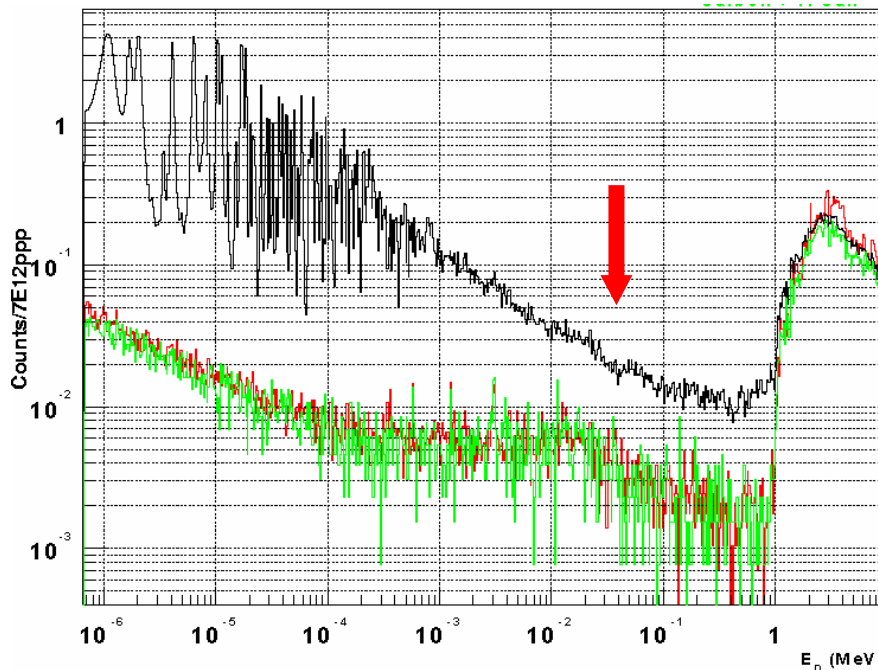


**Figure 7:** Signal-to-background ratio illustrated at the example of the raw spectra from the  $(n,\gamma)$  cross section measurement on  $^{151}\text{Sm}$  taken in 2002 at n\_TOF. The arrow indicates the energy range around 30 keV, which is the most relevant region for the astrophysical aspects of this cross section.

From the experimental side the necessary amount of sample material could have been reduced by a factor of 30, assuming that a signal-to-background ratio of unity is adequate and that the  $\text{C}_6\text{D}_6$  detectors, which were actually used, were replaced by the 10 times more efficient TAC. Thus, the measurement could have been performed with a sample of 5 mg at best.

In dealing with radioactive samples it is mandatory to reduce this limit further, since most of the isotopes of relevance for astrophysics are not available in milligram amounts and in order to keep the radiological hazards as low as possible, in particular for the actinide samples, which are of interest for technological applications. However, a further reduction of the sample mass and the corresponding increase in sensitivity can only be achieved by an increase in neutron flux. In this direction another factor of five would be gained by using a heavy water moderator, but by far the largest gain would result from a 10 times shorter flight path. In addition to the factor of 100 from the increased solid angle, the measurement would also benefit from the 10 times lower duty factor because the neutron burst is passing the sample in a correspondingly shorter time interval. Accordingly, a  $\text{D}_2\text{O}$  moderator and a flight path of 20 m would imply a fantastic enhancement of the experimental sensitivity by **a factor of 5000!**

This opens the possibility to perform measurements on samples of a few micrograms. Since samples of that mass can be accumulated at future RIB facilities in a few hours this improvement of the sensitivity implies a multitude of possibilities not only for measurements on *s*-process branch point isotopes but also on unstable isotopes related to explosive nucleosynthesis, e.g. to the aforementioned *r* process as well as to the *p* process, which is responsible for the origin of the rare proton-rich isotopes, and which occurs also in supernovae.

For measurements on actinide isotopes, there would be practically no more serious limitations due to the radiotoxicity of the sample. For instance, the necessary amount of  $^{241}\text{Am}$  could be limited to 10 micrograms corresponding to an activity of  $10^6$  Bq only. Even cross section measurements at yet shorter-lived actinide isotopes would be possible at such a short flight path, e.g. on  $^{238}\text{Pu}$ ,  $^{242}\text{Am}^m$  and  $^{242,243,244}\text{Cm}$ .

Also in the field of nuclear fission the high flux and still superb TOF resolution will allow one to perform much more comprehensive measurements covering the many facets of this complex reaction in a more adequate way.

In summary, an additional, short flight path at n\_TOF bears most exciting options for a completely new class of experiments and will be further investigated by detailed simulations and by studying the technical feasibility.

# CAPTURE STUDIES

## Introduction

Neutron capture reactions are of utmost importance for the neutron balance in stars and in nuclear reactors as well as for the quantitative understanding of the related stellar nucleosynthesis and of the production of hazardous nuclear wastes. A considerable part of the experimental program of the collaboration is motivated by these aspects, since n\_TOF provides unique possibilities for establishing reliable and accurate data for these applications. The proposals outlined below are based on the experience with previous experiments and are using the detection techniques developed during the first phase of n\_TOF. Some cases, however, are formulated under the assumption of the dramatically improved sensitivity that can be realized with a second, short beam line (see “The Second n\_TOF beam-line”, page 22).

## Nuclear Astrophysics

### **Stellar neutron capture cross sections of Mo, Ru, and Pd isotopes<sup>2</sup>**

n\_TOF offers optimal performance for neutron capture studies in nuclear astrophysics. The proposed measurements on the stable Mo, Ru, and Pd isotopes benefit particularly from the high neutron flux, the superb resolution in time of flight, the low intrinsic backgrounds, and the wide neutron energy range. The neutron capture cross sections of Mo, Ru, and Pd are required in two fields, for the interpretation of the isotopic patterns in presolar SiC grains and for the reliable determination of the *r*-process abundances in the critical mass region between Zr and Ba.

SiC grains are found in meteorites and originate from circumstellar clouds of AGB stars, which are highly enriched in fresh *s*-process material produced by these stars. They survived the high temperatures during the collapse of the proto-solar cloud and represent the most direct information [2] on the *s*-process efficiency of individual stars, an important constraint for current *s*-process models.

The abundances between Fe and the actinides are essentially built by neutron capture reactions in the *s* and in the *r* process. Since the *s*-process component can be reliably determined on the basis of accurate  $(n,\gamma)$  cross sections, the *r*-process counterpart is obtained by the difference,  $N_r = N_{\text{sol}} - N_s$  [3]. Recent spectral analyses of very old stars have shown that they contain essentially only *r*-process material and that the abundances of all elements heavier than Ba scale exactly as in the solar *r*-process pattern [4]. Below Ba this perfect agreement appears strongly disturbed. This could either indicate the operation of two independent *r*-processes or could simply be due to uncertain *s*-process abundances. The latter case can not be excluded at present, since the cross sections in this mass region exhibit large uncertainties. Hence, improved data will definitely be required to settle this exciting issue.

---

<sup>2</sup> *Contributed by:* M Heil, F Käppeler, and R Plag (Forschungszentrum Karlsruhe).

**Setup:** Practically all measurements can be performed at the existing flight path, mainly using the TAC. However, a few cases may need additional runs with the  $C_6D_6$  detectors if the neutron scattering background becomes too dominant.

**Samples:** All samples are stable and not hazardous in any respect. Metal samples are preferable, but if not available, the oxides are acceptable alternatives.

**Count-rate estimate (# of p):** Assuming sample masses of typically 500 mg, measuring times with the TAC of typically a few days will be sufficient. Accordingly,  $5 \times 10^{16}$  p are estimated for each of the 20 stable isotopes of Mo, Ru, and Pd.

### The s-process efficiency in massive stars<sup>3</sup>

About 50% of the elements beyond iron are produced via slow neutron capture nucleosynthesis (*s* process). Starting at iron-peak seed, the *s*-process mass flow follows the valley of stability since the time scale for beta decay is much faster than for neutron capture. In the vicinity of the Fe seed the resulting abundances are dominated by the weak *s*-process component, which is related to helium burning in massive stars of 10 to 25  $M_{\text{sol}}$  [5]. Only above Zr, the contributions from thermally pulsing low mass AGB stars begin to dominate the *s*-process abundances in the solar system [3].

The neutron exposure during the weak *s*-process is not strong enough that the so-called local equilibrium is reached, which implies different production rates for neighbouring nuclei. Accordingly, the neutron capture rate of a nucleus, which experiences the entire mass flow, will affect not only the abundance of that particular isotope, but the abundances of all isotopes in the following reaction chain and hence the overall *s*-process efficiency as well. That this behaviour depends critically on the cross sections of single isotopes near the Fe seed has been recently found in detailed nucleosynthesis calculations for a 25  $M_{\text{sol}}$  star [6]. In this work the role of important bottle-neck cross sections has been demonstrated at the example of  $^{62}\text{Ni}$ . The experimental cross section data showed obvious discrepancies, rather typical for most isotopes in this mass region. According to recent sensitivity analyses [7], it appears mandatory to re-measure **all Fe, Ni, Zn and Se isotopes** with much improved accuracy, using the unique features of the n\_TOF facility, i.e. high neutron flux, superb resolution in time of flight, low intrinsic backgrounds, and a wide neutron energy range. These results will eventually be the basis for settling the crucial problem of the contributions from massive stars to the abundance distribution in the universe.

**Setup:** Practically all measurements have to be performed with the  $C_6D_6$  detectors because of the huge neutron scattering background, which is expected for these resonance dominated cross sections. Since all cross sections in this group of

---

<sup>3</sup> *Contributed by:* M Heil, F Käppeler, and R Plag (Forschungszentrum Karlsruhe).  
*For the Se measurements:* Y Nagai (Osaka University), M Igashira, and T Osaki (Tokyo Institute of Technology).

isotopes are small, it is important to reduce the in-beam  $\gamma$ -ray background as discussed in the Section “Facility”.

**Samples:** All samples are stable and not hazardous in any respect. Metal samples are preferable, but if not available, the oxides are acceptable alternatives.

**Count-rate estimate (# of p):** Assuming sample masses of typically 200 mg, measuring times with the  $C_6D_6$  detectors of typically 10 days will be required. Accordingly,  $2 \times 10^{17}$  p are estimated for each of the 9 stable isotopes of Fe and Ni.

## Radioactive branch points and stellar neutron poisons<sup>4</sup>

Branchings in the reaction chain of the slow neutron capture process (*s* process) have been shown to represent invaluable diagnostic tools for the deep stellar interior [3]. Though beta decays are in general much faster than neutron capture reactions in the *s* process, which occur on a time scale of typically 1 yr, there are some 15 cases of beta unstable isotopes with sufficiently long half-lives that beta decay and neutron capture may compete. The resulting branchings are local phenomena as indicated in Figure 8 at the example of the branchings at  $A=147/148$ . The strength of a branching can be expressed in terms of the rates for beta decay and neutron capture of the branch point nuclei as well as by the  $\sigma N_s$  values of the involved *s*-only isotopes  $^{148}\text{Sm}$  and  $^{150}\text{Sm}$ , which stand for the corresponding parts of the reaction flow.

The key data for the analysis of a branching are  $(n,\gamma)$  cross sections of the stable *s*-only isotopes and of the radioactive branch point nuclei. While measurements on most *s*-only isotopes are available with the required accuracy of 1 to 2%, there is almost no experimental information for the radioactive branch points.

The type of information that can be deduced from branching analyses includes the neutron flux, temperature, pressure, and convective motions at the stellar site – crucial constraints for any *s*-process model. These constraints become even more stringent by the fact that the related parameters affect the various branchings in different ways, making the consistent description of all branchings an even more demanding task.

As was already demonstrated the extremely low duty factor makes the  $n$ -TOF facility ideally suited for measurements on radioactive samples [9][10]. In the course of these experiments it turned out that a reduction in flight path leads to an enormous increase in sensitivity. With this improvement, measurements on samples with masses in the  $\mu\text{g}$  regime will become possible, an essential step in reducing the radiation hazard associated with such measurements.

Based on experimental data taken in the measurement of the  $^{151}\text{Sm}$  cross section, it can be realistically expected to improve the sensitivity by four orders of magnitude if the water moderator is replaced by  $D_2O$  and if a second flight path of 20 m can be constructed perpendicular to the direction of the proton beam.

---

<sup>4</sup> Contributed by: M Heil, F Käppeler, and R Plag (Forschungszentrum Karlsruhe).

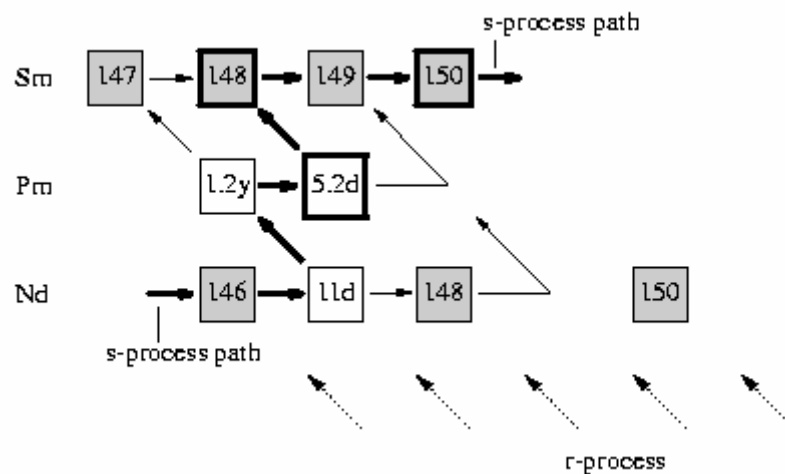


**Figure 8:** The *s*-process path between Nd and Sm is partly bypassing  $^{148}\text{Sm}$  due to the branchings at  $A = 147/148$ . The second *s*-only isotope,  $^{150}\text{Sm}$  experiences the full reaction flow. Note that both *s*-only isotopes are shielded against the respective *r*-process contributions by their stable isobars in Nd. The half-lives of the branching points reflect the stellar values [8].

The higher flux at a shorter flight path would also open new possibilities for measurements of very small cross sections, e.g. for the very light elements. In spite of their small cross sections this species has a strong influence on the stellar neutron balance simply because they populate the *s*-process site in very large abundances. The yet uncertain effect of these neutron poisons represents a pending problem, which needs to be addressed with improved cross sections.

**Setup:** Measurements on unstable targets should preferentially be performed with the TAC in order to achieve the optimal sensitivity required for investigations with very small amounts of sample material. For the neutron poisons the choice of setup depends on the particular case. However, both types of measurements will depend on the possibility to use a shorter flight path.

**Samples:** Unstable samples are potentially hazardous and should therefore be minimized in mass as far as possible. The radiotoxicity may vary and needs to be considered for each case individually. It is important to note that samples of branch point isotopes could possibly be produced on site at the ISOLDE facility.

**Count-rate estimate (# of p):** Measurements on extremely small samples require comparably more protons. Nevertheless, even such unique experiments should be possible with  $5 \times 10^{17}$  p per isotope.

## Nuclear waste transmutation & related nuclear technology studies<sup>5</sup>

The n\_TOF facility offers unique experimental conditions for performing neutron capture cross section measurements on highly radioactive samples of a few mg in mass as was demonstrated by the excellent n\_TOF results obtained with the TAC in 2004 [11][12].

The total absorption technique is a powerful tool for investigating the electromagnetic de-excitation of isotopic species independently from their particular de-excitation pattern. By summing over the complete  $\gamma$ -ray cascade emitted in neutron capture events, the TAC provides a clear peak in the  $\gamma$  spectrum corresponding to the neutron separation energy of the compound nucleus plus the energy of the captured neutron. Due to this unique signature capture events can be largely discriminated from all possible sources of background. Moreover, the segmentation of the TAC allows one to use  $\gamma$  multiplicity estimators for the separation of different reaction channels, particularly capture and fission on fissionable actinides. In addition, the use of beam time is highly optimized, since the TAC efficiency is close to 100%.

In measurements on small amounts of radioactive isotopes the TAC offers significant advantages over alternative techniques commonly employed in neutron capture cross section measurements such as the Moxon-Rae and the pulse height weighting (PHW) techniques:

- High efficiency of nearly 100% versus 0.1% for the Moxon-Rae detectors and 10% for the total energy detectors used for the PHW technique.
- Good energy resolution, which allows the recognition of structures in the energy spectra.
- Direct background suppression mechanisms based on combined analysis of multiplicity and total deposited energy.
- Systematic uncertainties associated with the counting efficiency are at the level of only 1%.

However, one of the major sources of background in neutron capture measurements with the TAC is related to its rather large neutron sensitivity. Neutrons scattered by the sample or additional dead materials inside the calorimeter have a non-negligible probability for being captured by the detector itself, mostly in the Ba isotopes of the scintillator crystals. The  $\gamma$ -ray cascade of such events can be hardly distinguished from a real capture event in the sample. While the neutron sensitivity of the n\_TOF carbon fiber C<sub>6</sub>D<sub>6</sub> detectors used for the PHW technique is smaller than 1/10000, the neutron sensitivity of the TAC is of the order of a few percent.

While the lowest neutron sensitivity would be obtained by using bare, self-supporting samples placed in the center of the TAC, the safety regulations at CERN

---

<sup>5</sup> *Contributed by:* E Gonzales Romero, D Cano-Ott (CIEMAT, Madrid), F Gunsing, and E Berthoumieux (CEA, Saclay).

required the actinide samples to be encapsulated in sealed, certified containers corresponding to the ISO 2919 standard. Since it was not possible to meet this requirement with an optimal design, the measurements in 2004 had to be carried out with samples of a few tens of mg encapsulated in Ti containers 500 mg in mass. As shown in Figure 9, this solution allowed still to perform precision measurements in the resolved resonance region. The region above 2 keV, however, is strongly handicapped by the scattering effect of the wide Ti resonances.

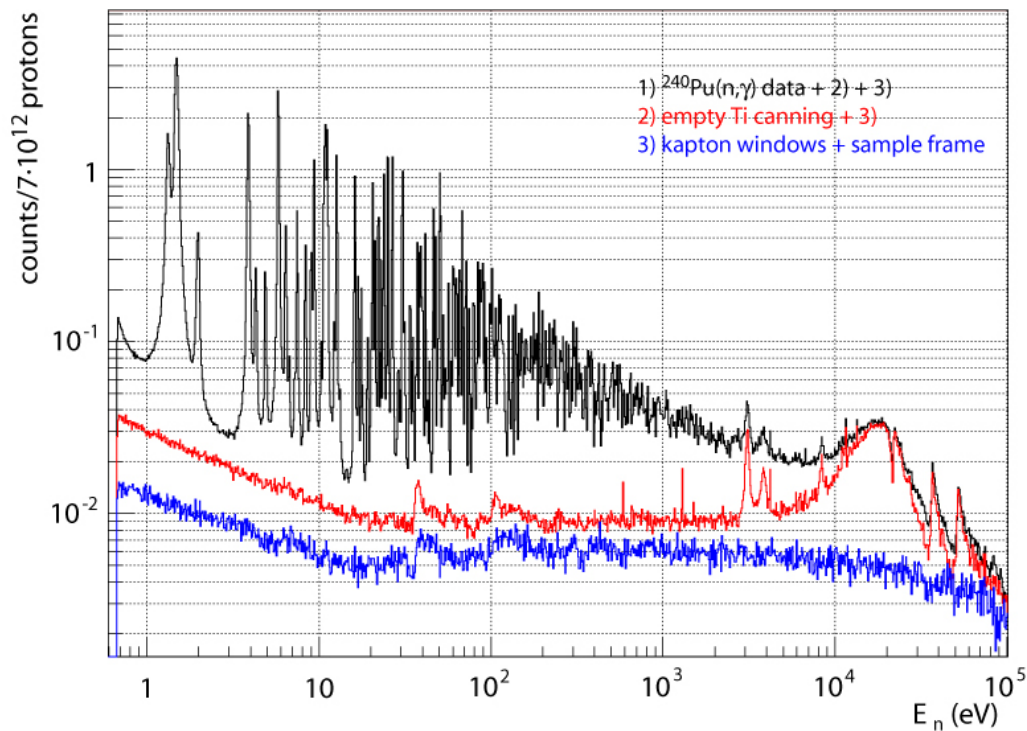


**Figure 9:** Raw counting rates for the  $^{237}\text{Np}$  measurement with the TAC at  $n\_TOF$  in the 2004 campaign and the background contribution from the Ti canning of the sample.

In future experiments, these problems can be largely avoided. Meanwhile a provider has been found which will deliver the samples in the optimized containers sketched in Figure 10. This design consists of 2 m long, evacuated, and ISO-certified containers with the actinide sample deposited on a very thin Al backing at the center. In this way, the dead material will be minimized and placed mostly outside the TAC, where it can be efficiently shielded. Based on Monte Carlo simulations it is expected that the background from scattered neutrons will be reduced by more than a factor of 10.

Alternatively, the samples can be delivered inside an ISO-certified mini-ionization chamber, thus allowing to perform simultaneous neutron capture and neutron induced fission cross section measurements. Such a technique will be required for measurements on fissile isotopes, i.e.  $^{239}\text{Pu}$  and  $^{245}\text{Cm}$ .

The preliminary list of experiments contains the  $(n,\gamma)$  cross section measurements on  $^{234,236,238}\text{U}$ ,  $^{242}\text{Pu}$ , and  $^{241,243}\text{Am}$  and the simultaneous  $(n,\gamma)$  and



(n,f) measurements with the mini-ionization chamber on  $^{233}\text{U}$ ,  $^{239}\text{Pu}$ , and  $^{245}\text{Cm}$ . The present problems with the capture cross sections of  $^{242}\text{Pu}$ ,  $^{241,243}\text{Am}$  and  $^{245}\text{Cm}$  were discussed in detail in the proposal “Measurement of the neutron capture cross section of  $^{233}\text{U}$ ,  $^{237}\text{Np}$ ,  $^{240,242}\text{Pu}$ ,  $^{241,243}\text{Am}$ , and  $^{245}\text{Cm}$  with a Total Absorption Calorimeter at n\_TOF”[11] submitted to INTC in 2003. Though the capture cross section of  $^{239}\text{Pu}$  has been repeatedly investigated so far, the proposed experiment is well motivated by the improved systematic uncertainties, which will provide an excellent validation of a capture measurement for a well documented fissile isotope. These results will be also important for the accurate correction of the  $^{239}\text{Pu}$  impurity in the  $^{240}\text{Pu}$  measurements of 2004.

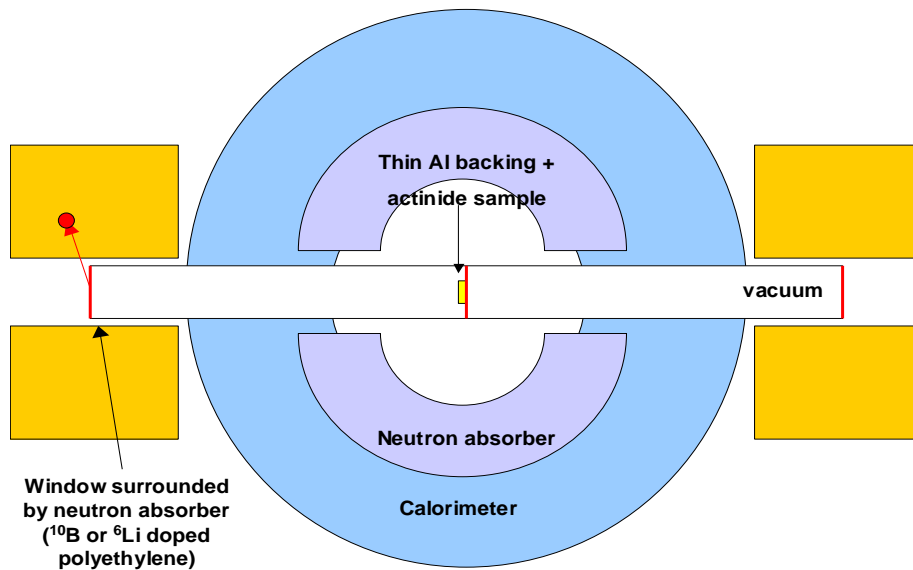


**Figure 10:** Low neutron sensitivity setup with long sealed containers.

A low mass canning, together with a fission veto, is necessary for accurate capture measurements and has been mentioned already. In addition, the TAC itself can be ameliorated, notably the sensitivity to the initial flash, the signal output of the voltage dividers, and the neutron sensitivity. Concerning the data acquisition system, an increased dynamic range of the flash ADCs would allow to include the very important thermal energy range in the time-of-flight measurements. Finally, several options are currently under investigation to eliminate the non-significant events from the data rate.

In view of the necessary commissioning periods for determining the neutron fluence, the time/energy relation, and the resolution function of the facility as well as the background measurements, the reference runs with a  $^{197}\text{Au}(n,\gamma)$  sample, and the neutron capture cross section measurement of each sample listed, a grand total of  $4 \cdot 10^{19}$  protons will be needed.

# NEUTRON INDUCED FISSION STUDIES

## Introduction<sup>6</sup>

Recently, several proposals have been made to reduce the radiotoxicity of nuclear waste containing Trans-Uranium elements (TRU). They all rely on neutron induced capture and fission of the TRU, in particular of  $^{237}\text{Np}$ ,  $^{241,243}\text{Am}$ , and  $^{244,245}\text{Cm}$ . It is clear that any kind of waste burner system, critical or sub-critical, thermal or fast, will need to be loaded with fuel containing a large fraction of TRU. The response of these systems (e.g. criticality conditions) to the presence of TRU is directly linked to the fission and capture cross sections of the mentioned TRU isotopes. The fission cross sections of TRU are therefore fundamental elements in assessing the strategy to be followed in detailed feasibility studies of nuclear waste transmutation.

A peculiarity of the fission process in the higher actinides in consideration here (with the exception of  $^{245}\text{Cm}$ ) is that they have a relatively high fission threshold, above a few hundred keV. This is one of the considerations which led to the proposal for accelerator driven systems (ADS) [13], in which a fast neutron spectrum is considered for transmutation. In addition, in some advanced fuel cycle scenarios the contribution of  $^{237}\text{Np}$  and  $^{241}\text{Am}$  to the total fission rate can be as large as 10% [14] and the fraction of sub-threshold fission typically of 5% even in a fast spectrum. Therefore, both below and above threshold these isotopes provide important contributions to the global reactor neutron balance. In the case of  $^{245}\text{Cm}$ , fission represents nearly 90% of the neutron absorption in fast neutron spectra, and its contribution to the global fission rate is expected to be larger than 6% in some ADS fuelled with minor actinides. Direct fission is the most important channel for the transmutation of these isotopes. Furthermore, the fission cross sections play an important role for the precise definition of the isotopic composition of ADS transmuted fuel.

From these considerations it appears that for the design and operation of such advanced systems it is necessary to extend the measurements of accurate fission cross sections to a much wider neutron energy range as for thermal systems, covering the region up to at least several MeV. The fission threshold and the sub-threshold resonance structure in some of the higher actinides allow for studies of the outer fission barrier, as well as of the structure (hyper-deformation) of the fission potential. The very high resolution of the n\_TOF beam provides a unique opportunity to address some of the open questions concerning the structure of sub-threshold vibrational resonances as already shown in the  $^{234}\text{U}(n,f)$  measurement performed in 2002.

With these basic motivations, it is proposed to perform neutron induced fission cross section measurements using the CERN n\_TOF facility. The neutron beam characteristics and experimental conditions at n\_TOF are optimal for measurements of fission cross sections on radioactive materials. The results obtained during the 2002, 2003 and 2004 measurement campaigns provide the necessary

---

<sup>6</sup> For the general motivations on fission nuclear data needs and state of the art see: INTC-P177, April 2003.

confidence in the operation of the fission detectors and on the achievable accuracy in a wide energy range  $1 \text{ eV} \leq E_n \leq 250 \text{ MeV}$  (and, in principle, up to 1 GeV).

## Measurement of the $^{235}\text{U}$ fission cross section up to 150 MeV <sup>7</sup>

During the n\_TOF measurement campaigns in the years 2002-2004 a large body of data on the fission cross-section of minor actinides relative to the fission cross section for  $^{235}\text{U}$  and  $^{238}\text{U}$  has been collected in the neutron energy range from thermal to 200 MeV. In addition, the analysis of the  $\gamma$ -multiplicity data that were obtained from the TAC measurements in 2004 on minor actinides allows to deduce the capture to fission cross section ratio  $\alpha = \sigma_f / \sigma_c$ . Normalizing these data to the known standard, for example to the  $^{235}\text{U}$  fission cross section, one can obtain absolute cross-sections of fission and capture in the neutron energy up to 20 MeV. At higher energies a reliable standard cross section is yet missing. Though several measurements of fission cross-section ratios have been reported, the discrepancies in the data exceed the statistical uncertainties by far and need to be resolved (Figure 11).

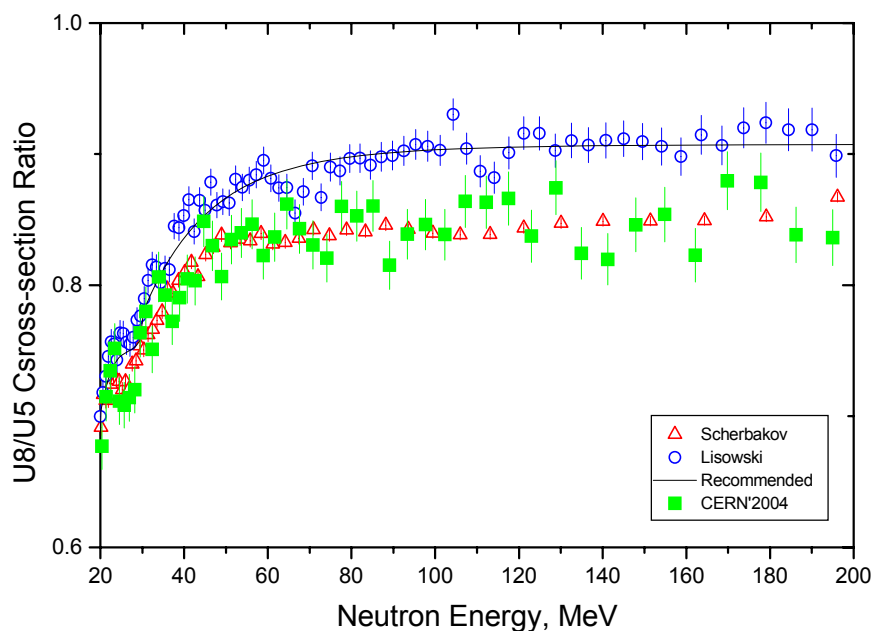


**Figure 11:** Fission cross section ratio of  $^{238}\text{U}$  to  $^{235}\text{U}$  obtained at n\_TOF in 2004 in comparison with previous data.

Besides the problem of the cross section standard, the high neutron energy resolution of n\_TOF revealed the resonance-like structure of the  $^{235}\text{U}$  fission cross section even in the energy region above 2.5 keV, where the recommended  $^{235}\text{U}$  cross section exhibits an almost smooth behavior (Figure 12).

<sup>7</sup> Contributed by: W Furman (JINR, Dubna), A Goverdowski (IPPE, Obninsk), V Konovalov (JINR, Dubna), and V Ketlerov (IPPE, Obninsk).

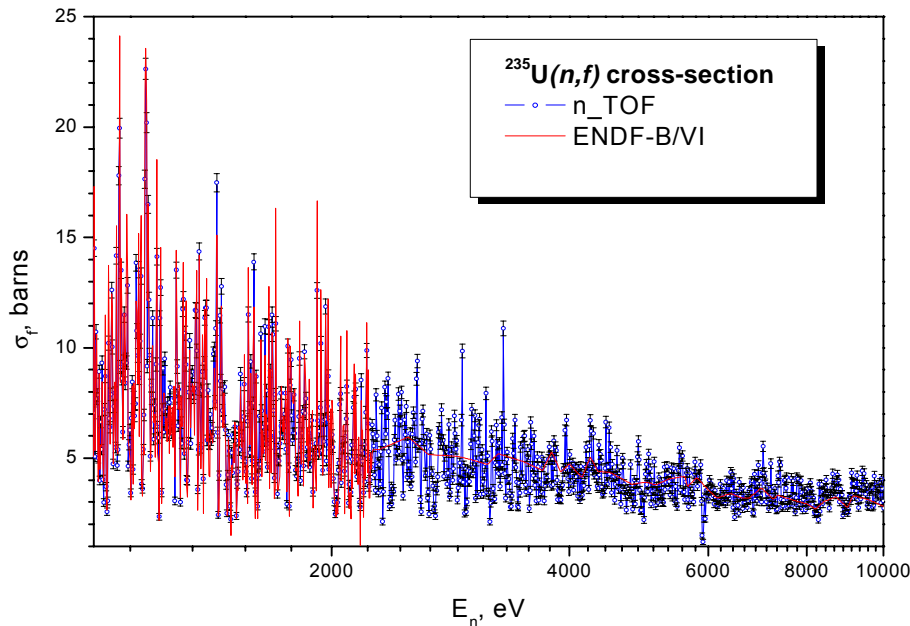


**Figure 12:** The extremely high energy resolution obtainable at n\_TOF illustrated by the measured fission cross section of  $^{235}\text{U}$ .

Accordingly, the  $^{235}\text{U}$  fission cross section must be measured relative to an independent standard with correspondingly good resolution in order to deduce the full information from capture and fission cross section data measured at n\_TOF from 2002-2004.

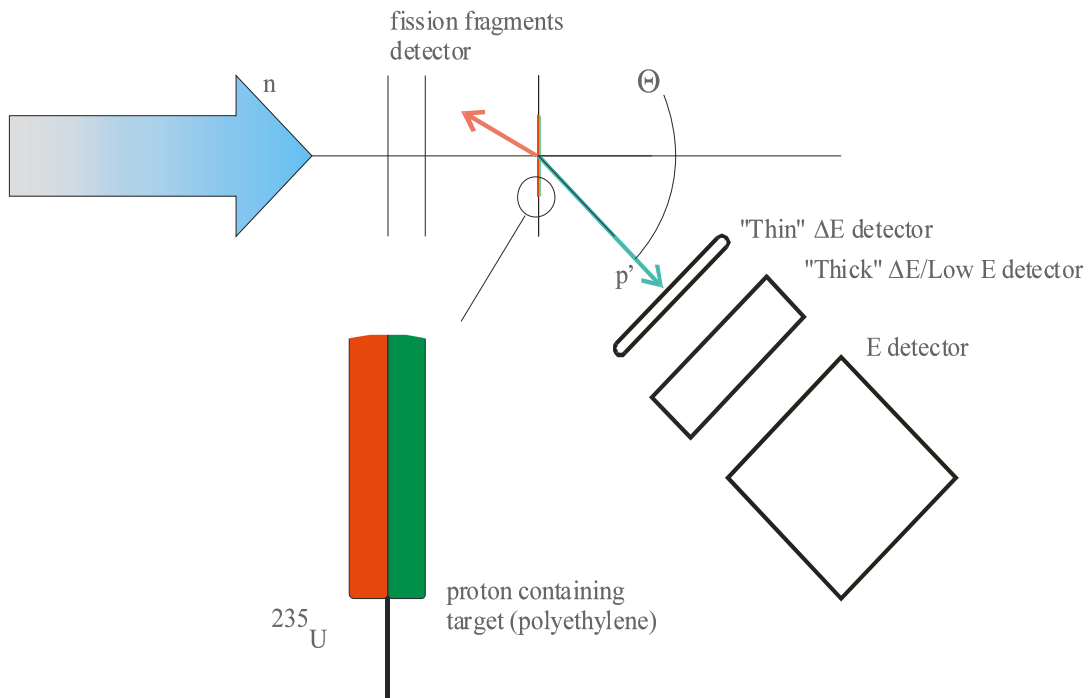
We propose to use the well known differential cross section of the reaction  $p(n,p')$  as such an independent standard. The measurements could be done with a proton recoil  $\Delta E/E$  telescope installed at a fixed angle  $\Theta$  relative to the beam. The energy of the incoming neutron can be determined by time-of-flight and that of the outgoing proton by absorption or time-of-flight using the “ $\Delta E$ ” detector for the start and the “E” detector for the stop signal. To enhance the energy range of the detected recoil protons a third detector could be added, which works as total absorber at relatively low energies and as an additional “ $\Delta E$ ” detector at higher energies, where the ionization losses over unit of distance are relatively small.

The ionization chamber with the  $^{235}\text{U}$  sample will be installed “back-to-back” with the proton target as sketched in Fig. 13. A MICROMEGAS detector or a parallel plate ionization chamber can be used as  $\Delta E$  detector, whereas the “thick  $\Delta E$ ” device can be a scintillation or a thin semiconductor detector.

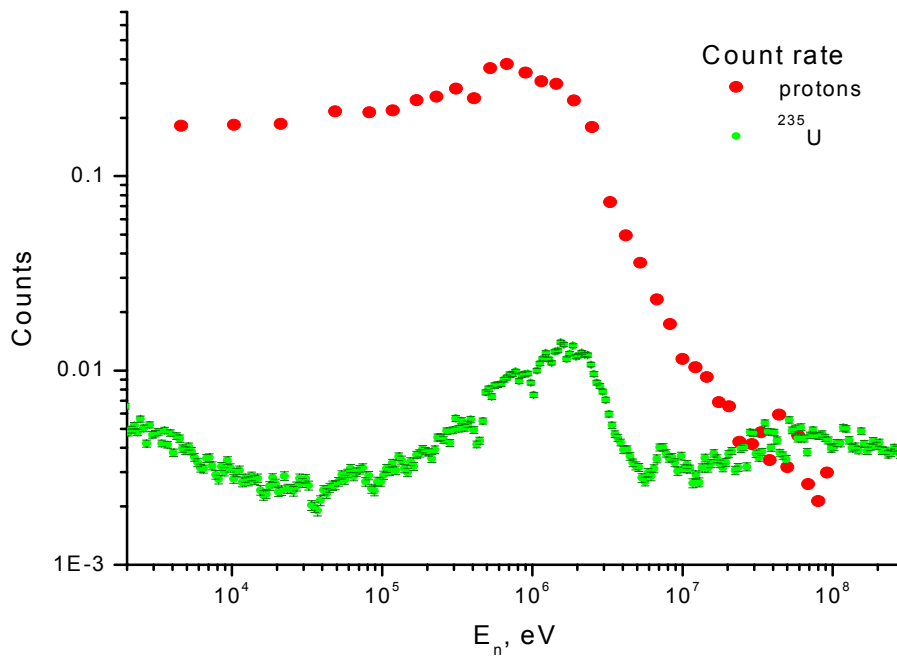
Figure 14 compares the simulated count rate for the recoil protons and the experimental  $^{235}\text{U}$  count rate (per accelerator burst of  $7 \cdot 10^{12}$  protons), which was obtained during the capture campaign in 2004. The data are presented with a resolution of 50 bins per decade. The  $^{235}\text{U}$  spectrum was taken with a sample of 5 mg, the diameter of the collimator was 2 cm, and the detector was located in the neutron escape lane at a flight path of 197 m. The parameters for the simulation of the recoil protons are summarized in Table 1.

Table 1: Parameters adopted for the simulation of the proton recoil spectrum plotted in Figure 14.

Beam radius	20 [mm]
Scattering angle	30 [degrees]
Target thickness	250 [ $\mu\text{g}/\text{cm}^2$ ]
Target to detector distance	250 [mm]
Detector radius	20 [mm]



**Figure 13:** Schematic layout of the proposed experiment.



**Figure 14:** Expected count rates per proton bunch of  $7 \cdot 10^{12}$  protons.

The simulation confirms that the count rate of the proton telescope is rather favorable up to 20 MeV and is still comparable to the fission rate up to 150 MeV.

## Fragment Distributions of Vibrational Resonances at the Fission Barrier <sup>8</sup>

Several heavy nuclei like  $^{232}\text{Th}$  and  $^{234}\text{U}$  have attracted high scientific interest for what was termed the “thorium anomaly” 20 years ago. This effect is connected with an additional splitting of the outer fission barrier resulting in a triple-humped structure and the corresponding exotic long lived hyper-deformed nuclear states. To carefully study this effect we propose to measure the angular and mass distribution of fission fragments emitted in the sub-barrier vibrational resonances with the aim to search for the coupling between compound states in the second well and vibrational resonances as well as for a connection between these resonances and the fission modes. For simultaneous measurements of the mass and angular distribution we propose the experimental setup sketched in Figure 15.

A thin target is located in the center of the detector at an angle of 45 degrees relative to the beam axis. The angular distribution of the fission fragments is measured by a cylindrical fast position-sensitive detector (preferably a set of semiconductor detectors or detectors of the Micromegas type). This detector determines the kinetic energy of both fission fragments - and hence their mass ratio -

---

<sup>8</sup> *Contributed by:* W Furman (JINR, Dubna), A Goverdowski (IPPE, Obninsk), V Konovalov (JINR, Dubna), and V Ketlerov (IPPE, Obninsk).

via time-of-flight. The “Start” signal for the fragments and the time mark for neutron time-of-flight spectrometry are obtained from a time-tag detector that should be transparent for the fission fragments.

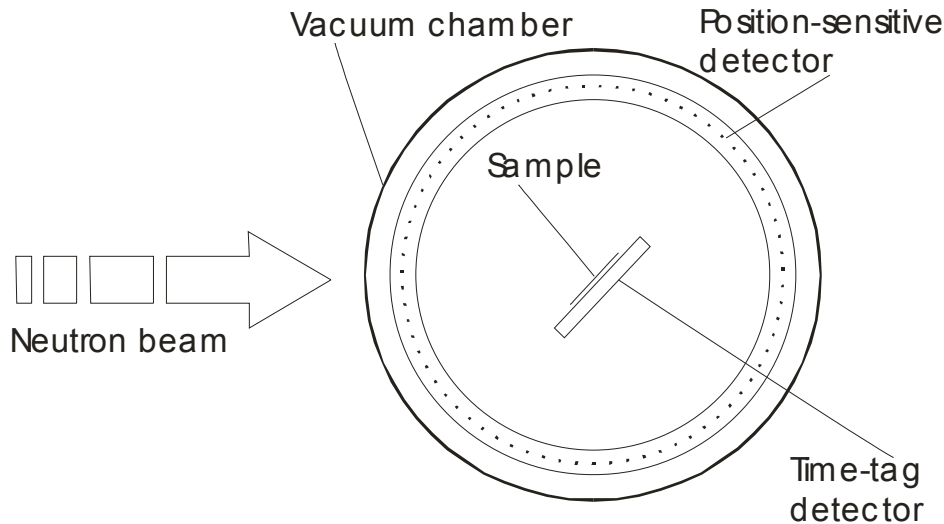


**Figure 15:** Setup for the measurement of mass and angular distributions of fission fragments.

In Figure 16 we show the expected count rate per pulse of  $7 \cdot 10^{12}$  protons for a 5 mg  $^{234}\text{U}$  sample located at a flight path of 20 m. The binning is chosen to be 200 bins per decade ( $\Delta E/E \approx 1\%$ ) that corresponds roughly to the intrinsic resolution of the n\_TOF facility at this distance. Since the double-differential (mass and angle) distributions for each energy bin should be determined with an accuracy of about 3% ( $\approx 1000$  counts) and since 25 points in angular distribution and 20 points in the mass distribution are to be achieved (to distinguish between Standard 1 and Standard 2 fission modes), about 500000 counts per bin are required at the mid point of the barrier. Thus, about one million proton bunches or  $7 \cdot 10^{18}$  protons are required for this experiment.

The feasibility of such comprehensive multi-parameter studies of neutron induced fission with high energy resolution illustrates again the enormous potential of a 20 m station, which will to obtain completely new information on the basic mechanisms of nuclear fission.

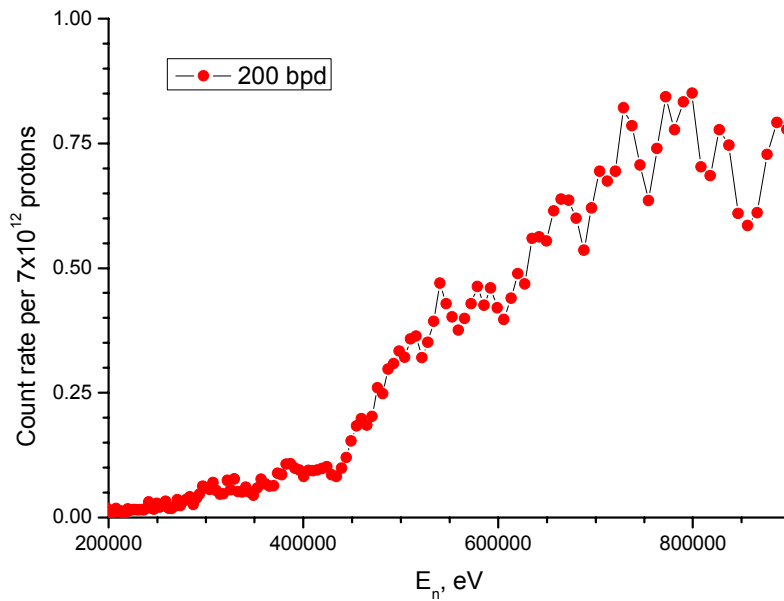


**Figure 16:** Expected integral count rate for a 5 mg  $^{234}\text{U}$  sample at the 20 m flight path.

## Fission cross sections and related measurements with PPACs detectors<sup>9</sup>

During the 2001-2003 period fission cross section measurements have been carried out with a setup based on Parallel Plate Avalanche Counters (PPAC). The measured isotopes are  $^{233}\text{U}$ ,  $^{234}\text{U}$ ,  $^{232}\text{Th}$ ,  $^{237}\text{Np}$ , and also  $^{209}\text{Bi}$  and  $^{\text{nat}}\text{Pb}$ , which fission only at incident neutron energies above 20 MeV. Figure 17 shows an example of the cross section obtained in the case of  $^{234}\text{U}$ . For this isotope one sees that it is possible to cover the entire energy range available at n\_TOF, from the resonance region up to the spallation domain (1 eV - 1 GeV).

$^{231}\text{Pa}$  is one of the important long lived wastes ( $t_{1/2}=32,000$  yr) in the thorium cycle where it builds up by (n,2n) reactions on  $^{232}\text{Th}$ . This isotope exhibits strong vibrational resonances in the fission cross section, which are helpful to explore the potential landscape along the deformation path. The main difficulties for the  $^{231}\text{Pa}$  cross section measurement related to the manufacturing of the target, to the availability of the sample and the complicated chemistry involved in its preparation can be solved by IPN-Orsay, where the radiochemistry group can produce a well-conditioned target.

---

<sup>9</sup> *Contributed by:* L Tassan-Got, C Stephan (IPN, Orsay), I Duran, and C Paradela (Universidade de Santiago de Compostela).



For highly radioactive isotopes the feasibility of the measurement is constrained by the low mass of the target (which is a consequence of the sample availability), the alpha background in the detectors, and the radiation protection conditions. If the second experimental area (**EAR-2**) will be available, measurements of such highly radioactive isotopes will be feasible. Even a measurement on  $^{241}\text{Pu}$  ( $t_{1/2}=14$  yr), which is highly fissile and becomes increasingly important for plutonium multi-recycling of the fuel, will be possible.  $^{244}\text{Cm}$  ( $t_{1/2} = 18$  yr) would be another case, although less relevant in the scope of waste incineration. Also, the  $^{241}\text{Am}$  and  $^{243}\text{Am}$  isotopes which could not be measured during the previous experimental campaigns could be reconsidered for a measurement in EAR-2 (Class-A Lab).

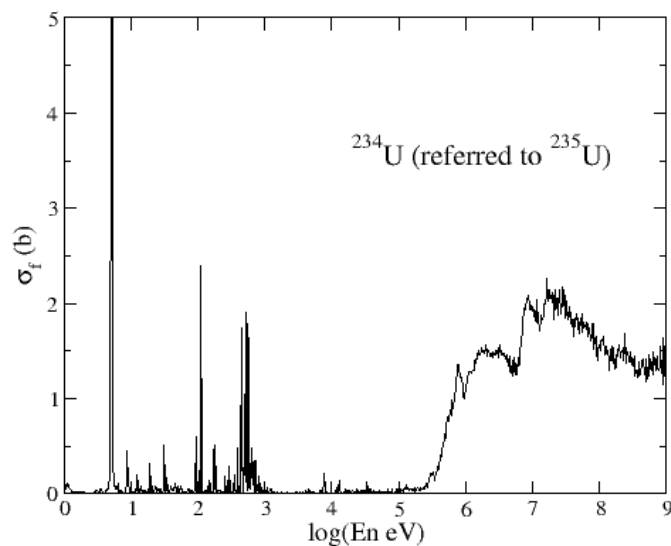


**Figure 17:** Fission cross section of  $^{234}\text{U}$  in the neutron energy range from 1 eV to 1 GeV measured at n\_TOF.

### Fission-fragments angular distributions

Below 100 keV neutron energy fission cross sections are dominated by s-waves and the angular distribution of the emitted fission fragments is generally isotropic. However in the threshold region strong anisotropies related to vibrational resonances can show up as illustrated at the example of Figure 18 illustrating the rapid variation of the anisotropy with neutron energy for the case of  $^{232}\text{Th}$  [15]. Surprisingly, this anisotropy persists up to at least 100 MeV and is stronger for incident neutrons than for incident protons [16].

Although the angular distributions have been measured up to a few MeV for several isotopes, only  $^{232}\text{Th}$  and  $^{238}\text{U}$  were investigated at higher energies. Angular distributions are important not only for the understanding of the fission process but also for the measurement of fission cross sections, because experimental setups exhibit generally angle-dependent efficiencies and are, therefore, sensitive to the anisotropy.

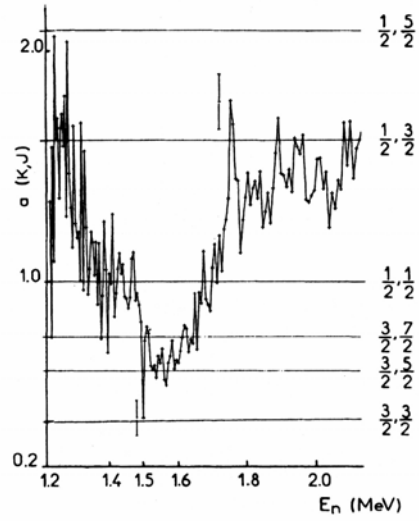


**Figure 18:** Energy dependence of the angular anisotropy in the fission of  $^{232}\text{Th}$  [15].

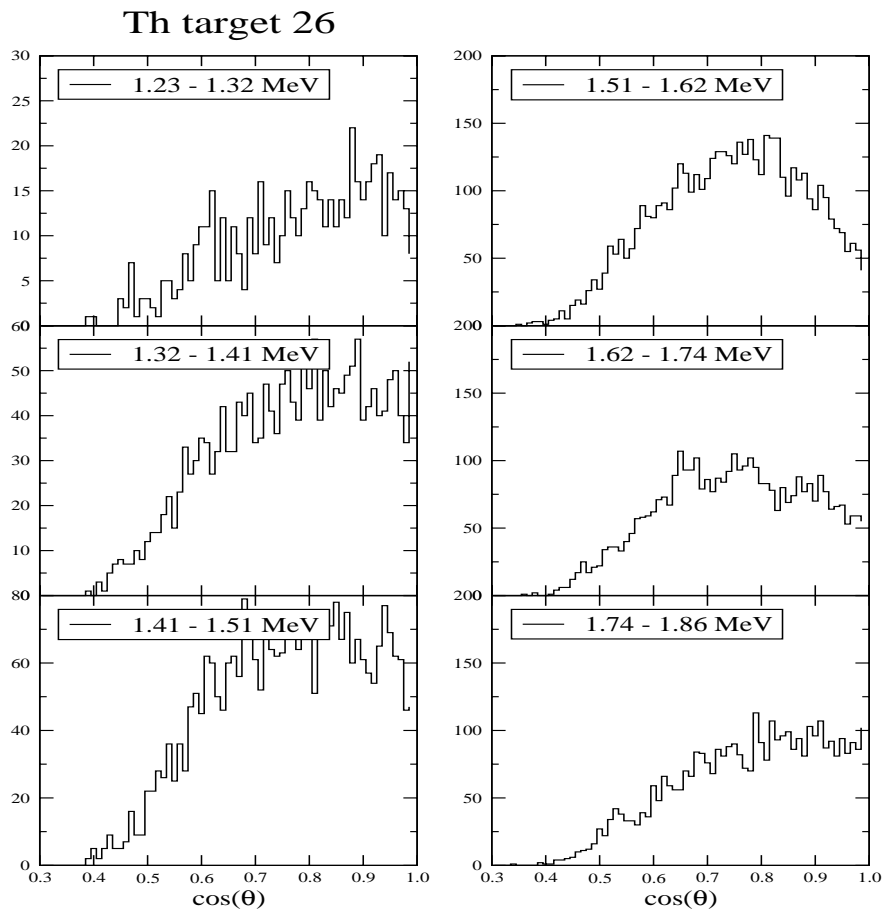


**Figure 19:** Variation of the fission-fragments angular distribution with incident neutron energy for  $^{232}\text{Th}$ .

With the experimental setup used in 2003 we were able to reconstruct part of the fission-fragments angular distribution by tracking. Figure 19 shows the inversion of the anisotropy in case of  $^{232}\text{Th}$  for six small energy bins. Up to a few MeV the extracted anisotropies and their energy variations are consistent with those measured in the past. We propose to measure more accurately, in the EAR-1 experimental area, the angular distributions of the isotopes already measured in 2003 by adapting the experimental setup. We plan to tilt the targets by  $45^\circ$  respect to beam axis. For the detector arrangement we study two possibilities: (a) Detectors parallel to targets or (b) Detectors parallel and orthogonal to the beam axis. The second option would allow to obtain a larger angular coverage, whereas the first would accommodate more targets.

## Fission-fragments yields

One of the key information to fully understand the fission process is the understanding of the Fission-Fragment (FF) yields. Unambiguous identification of FF both in charge and mass, on an event-by-event basis, is not an easy task. Mass distributions of FFs have been extensively measured at low energies (see e.g. [17]). A recent experiment in inverse kinematics at GSI [18] has investigated the FF yields of heavy-exotic nuclei induced by Coulomb excitation. In this experiment the mass and charge of the fission residues could be determined, but the resolution in excitation energy was rather limited.

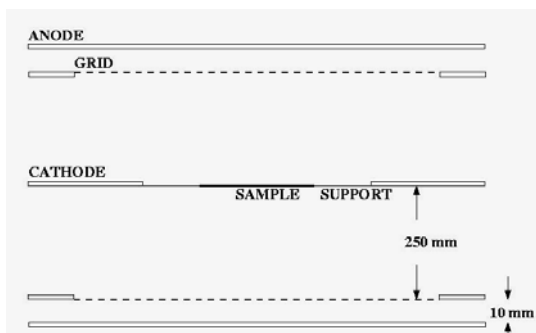


**Figure 20:** Electrode layout.

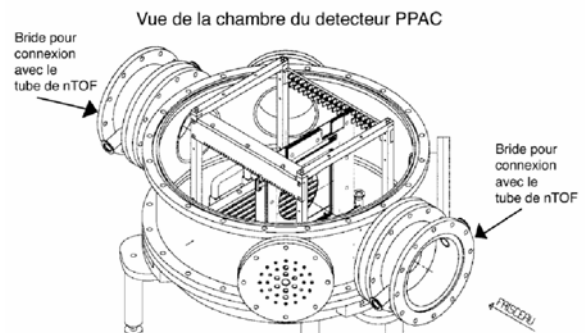


**Figure 21:** PPAC reaction chamber.

We proposing to measure a series of FF mass and charge distributions, taking advantage of the unique features of the n\_TOF facility and the advanced performance of ionization detectors. During the last years started to develop a procedure for obtaining charge as well as mass information from the FF signals in a twin ionization chamber. Figure 20 shows the layout, which is an improved design of the twin ionisation chamber proposed in [19] where the electrodes are rearranged in order to optimise the resolution, and which is to be installed in the PPAC reaction chamber (Figure 21). To validate the procedure we have analysed some FF data from a recent measurement of a Cf sample in a twin chamber at IRMM, Geel [20]. We developed appropriate software tools to analyse the fast-ADC signals from both sides of the twin chamber, taking advantage of the fact that both FFs are emitted in opposite directions. The simultaneous measurement of ranges, angles, and deposited

energies (Figure 22) allow us to correct for the energy-loss in the sample backing (Figure 23) and to determine both charge as well as mass of the emitted FFs.

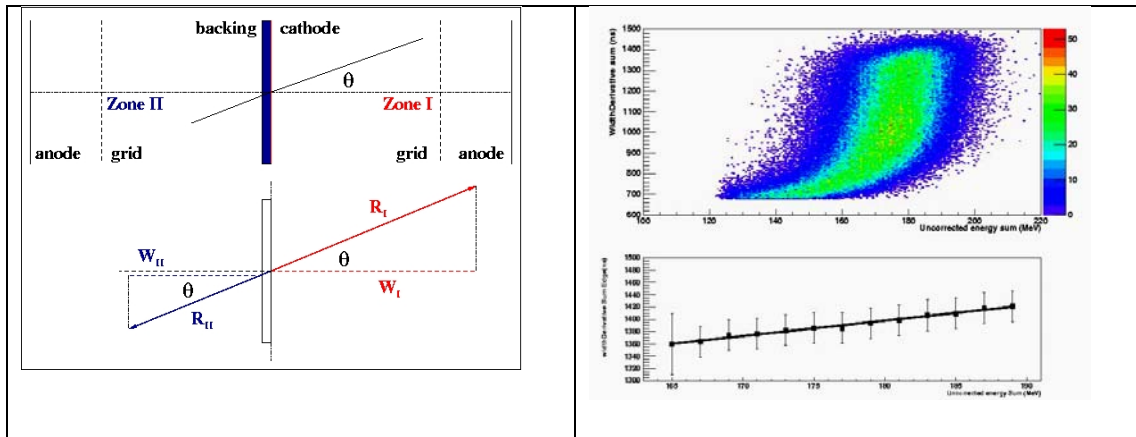


**Figure 22:** The polar angle is deduced by measuring different timing parameters.

In the experiments we are proposing we will first verify the method by measuring the well studied U samples and will then apply this technique to the other available samples, for which the FF yields are not well known. With a modified PPAC reaction chamber we expect to increase the resolution by reducing the gas pressure and by improving the electrode configuration with segmented anodes.

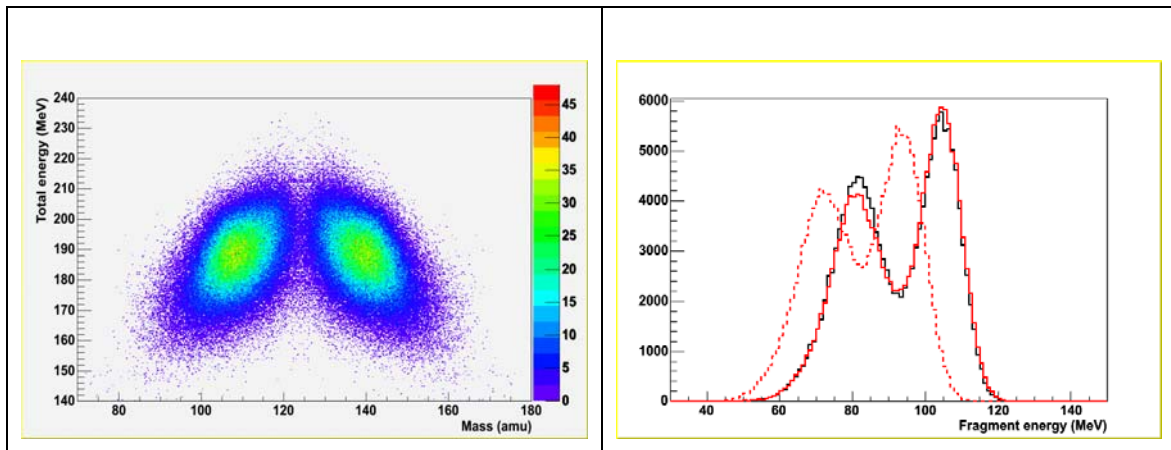


**Figure 23:** Energy and mass distributions after correction of energy losses.

## OTHER REACTIONS

In addition to the basic  $(n,\gamma)$  and fission cross section measurements, there has been a strong interest to perform measurements of cross sections for other neutron induced reaction channels. These are described here below with an introduction on the motivations and interest for basic studies in Nuclear Astrophysics and Nuclear Technologies. Several detection systems could be used at n\_TOF, both in the present EAR-1 as well as in the proposed EAR-2.

### $(n,p)$ , $(n,\alpha)$ , and $(n,xc)$ reactions

The largest nuclear physics uncertainties in  $p$  process and other high-temperature astrophysical environments are rates for reactions involving  $\alpha$  particles. Traditional methods for improving the  $\alpha$ +nucleus optical potentials, such as elastic scattering of  $\alpha$  particles, are of limited value because the measurements must necessarily be made at energies much higher ( $\sim 20$  MeV) than the energy range of relevance for astrophysics ( $\sim 10$  MeV)[21]. Hence, a potential for use in astrophysics can be extracted from these data only by largely unconstrained extrapolations.

Measurements of low-energy  $(n,\alpha)$  cross sections appear to be the best way to obtain the needed potential and hence to constrain the  $\alpha$ -particle rates for astrophysics. The  $Q$  values for these  $(n,\alpha)$  reactions are such that the relative energy between the  $\alpha$  particle and the residual nucleus are directly in the energy range of astrophysical interest, so that an extrapolation is not required. In addition, scaling the sample size to that employed in a previous measurement, using predicted cross sections, we calculate that as many as 30 nuclides across a wide range of masses from S to Hf are accessible to measurements at n\_TOF.

Besides the astrophysical goal it is very important to measure the  $\alpha$  widths of neutron resonances over a wide energy range. This would allow the comparison of the measured fluctuations of averaged  $\alpha$  widths with predictions of statistical theory. A previous measurement [22] over a more limited energy range had hinted at a possible non-statistical behavior in the averaged  $\alpha$  widths. The new data presented by Koehler *et al.* [23] show that the extracted  $\alpha$  widths exhibit fluctuations different from the expected behavior. Light charged particles generated in neutron induced  $(n,xc)$ -reactions yield important information on the reaction mechanisms and provide experimental constraints for nuclear model calculations. They have significant impact on the design of nuclear facilities (e.g. ADS and fusion reactors) as they result in gas production and subsequent embrittlement of materials.

At present, experimental data are rather scarce and were primarily obtained at mono-energetic neutron sources. The study of  $(n,xc)$ -reactions in the energy range between 1 and 100 MeV should be feasible at n\_TOF. In general, the neutron intensity per energy bin will be less than the neutron flux at comparable mono-energetic sources (e.g. the TSL at Uppsala or the CRC at Louvain-la-Neuve) but the reaction cross sections will be measured over the whole energy range simultaneously and under identical conditions.

Cross section measurements of light charged particle emission will result in a plethora of experimental data comprising integral production cross sections as

functions of incident neutron energy, double differential cross sections, and energy distributions of the light charged particles. With a state-of-the-art detector setup it is possible to distinguish the emitted protons, deuterons, tritons, He-3, and  $\alpha$ -particles.

In ADS these data are also of importance to estimate the amount of (radioactive) gas production in the facility for its effects on structural materials and the environmental output.

## Detection systems 1: Compensated Ion Chamber (CIC)<sup>10</sup>

At the University of Lodz a new compensated ion chamber (CIC) has been built, which allows to use higher gas pressures and bias voltages as well as twice as much sample material compared to the chamber used for the measurements at ORELA [24]. In particular, higher bias voltages allow the use of faster gases, resulting in an even better suppression of the  $\gamma$ -flash. The new detector also has better signal connectors and consists of high purity materials and will, therefore, exhibit inherently lower backgrounds. The increased gas pressure has the advantage that four compensated ion chambers can be accommodated in the detection volume of 11.5 dm<sup>3</sup> instead of two in the previous version. In spite of the narrower spacing, the distance between the electrodes will be larger than the range of the emitted alpha particles, providing even spectroscopic information although with limited resolution.

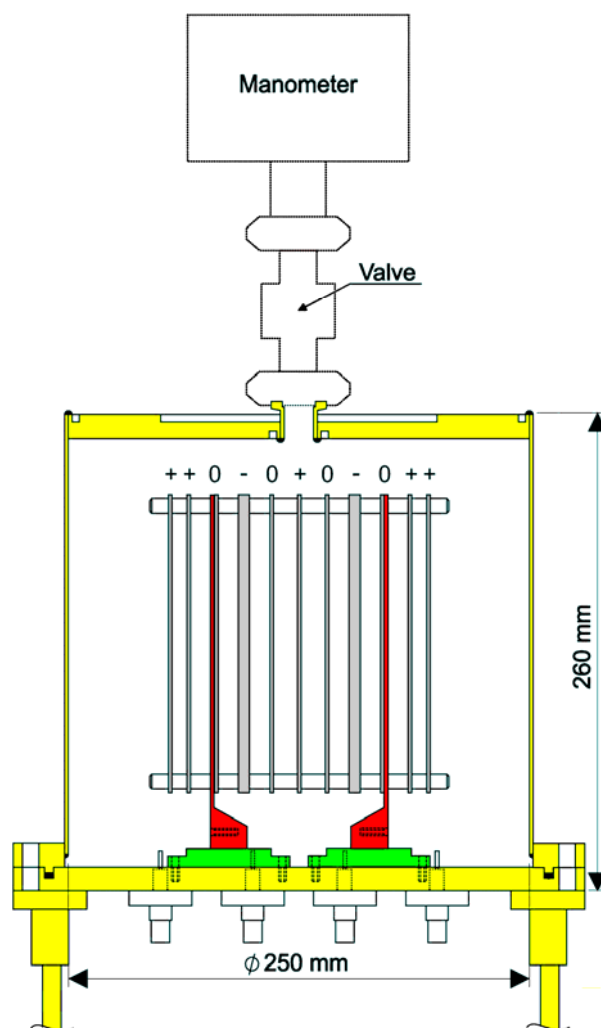


**Figure 24:** A schematic view of the new CIC.

<sup>10</sup> Contributed by: J Andrzejewski (University of Lodz), Yu M Gledenov (JINR, Dubna), PE Koehler (Oak Ridge National Laboratory), J Marganiec (University of Loz), and J Perkowski (University of Loz).

As a tune up experiment with our new CIC we propose to measure the  $^{147}\text{Sm}(n,\alpha)$  cross section over a period of 7 days using two  $^{147}\text{Sm}_2\text{O}_3$  targets of  $5\text{ mg/cm}^2$  thickness and 95.3 % enrichment as well as  $^6\text{LiF}$  targets for calibration runs for normalizing the raw counts to absolute cross sections. The samples will be 11 cm in diameter. We have evaluated the reaction rate per burst and conclude that the count rates at 185 m flight path should be 10 times smaller than obtained in our experiment at the shortest ORELA flight path of 8.83 m [24]. With a new 20 m flight path at  $90^\circ$  to the n\_TOF proton beam (**EAR-2**) the count rates should increase by a factor of 100, ten times higher than during the experiment at ORELA, where count rates of 34 1/h and 15 1/h were achieved for the strongest resonances at 3.4 eV and 184 eV, respectively. If the tune up experiment is successful, we plan to measure the  $(n,\alpha)$  cross sections of  $^{67}\text{Zn}$  and  $^{99}\text{Ru}$ .

## Detection systems 2: MICROMEGAS<sup>11</sup>

MICROMEGAS is a gaseous detector based on a simple geometry with planar electrodes [26]. This detector initially developed for tracking in high-rate, high-energy physics experiments but has been also used successfully as a neutron detector. Thanks to its high resolution to charged particles the detector with a converter as  $^6\text{Li}$ ,  $^{10}\text{B}$  or  $^3\text{He}$ , is suitable for neutron flux measurements and for neutron spectroscopy. Recent experiments in CEA, Saclay with a  $^{241}\text{Am}$  alpha source gave a resolution of about 2% for 5.4 MeV alpha particles. The MICROMEGAS detector can be used for  $(n,p)$  and  $(n,\alpha)$  cross section measurements at the n\_TOF facility at CERN. It has already been used in the n\_TOF neutron beam for the flux and the beam profile measurements.

The element under study can be used in the form of a thin foil with thickness of a few micrometers. This foil should be attached to the inner face of the drift electrode of the detector, acting as a neutron to charged particle converter. The produced protons or alpha particles are measured efficiently. As an example we take the case of  $^{58}\text{Ni}(n,p)^{58}\text{Co}$  reaction with a  $Q=0.9\text{ MeV}$ . The threshold of the reaction is about 2 MeV and the energy of the proton depends linearly on the neutron energy up to 20 MeV. As a matter of fact, the proton spectroscopy can provide the neutron spectrum. The count rate depends on the cross section of the reaction for each isotope. In most cases the cross section is between 50 mbarns and 500 mbarns. For a target with 5cm of diameter and 1 $\mu\text{m}$  of thickness the count rate is estimated to be of the order of 1 reaction/pulse.

---

<sup>11</sup> *Contributed by:* S Andriamonje (CEA, Saclay), and I Savvidis (Aristotle University of Thessaloniki).



### Detection systems 3: $\Delta E$ -E telescopes<sup>12</sup>

A new scattering chamber will be designed and installed. Detector telescopes ( $\Delta E$ -E or  $\Delta E$ - $\Delta E$ -E) will be placed within the evacuated scattering chamber at several angles around the sample (whose surface normal is rotated  $45^\circ$  out of the beam direction). Silicon detectors or plastic scintillators may be employed as  $\Delta E$  detectors. Usually a CsI(Tl) scintillation detector is used as E detector. Alternatively, the use of silicon detectors may be considered. We propose to place telescopes at 3-5 emission angles and consider a set of up to 6 telescopes per emission angle.

The neutron energy will be determined by time-of-flight with time information derived from the telescopes. The charged particles will be identified by their energy loss in the  $\Delta E$  detectors and by pulse shape analysis of the signals generated in the CsI detectors. A neutron beam monitor has to be installed to provide an independent flux determination. In the energy range of interest this can be done by uranium fission chambers and/or proton recoil telescopes.

Assuming a sample ( $A \sim 60$ ) thickness of  $10 \text{ mg/cm}^2$  and an average  $(n,xc)$ -cross section of 50 mb one expects at the nominal neutron flux of the n\_TOF facility (with the large diameter of the 2<sup>nd</sup> collimator) the emission of 15 charged particles per pulse over the whole energy region of interest. Due to the low count rate it would be advisable to operate the charged particle measurements in combination with fission experiments. Due to the required coincidence no significant background is expected.

We propose to start with samples where experimental data are already available (e.g. Fe-56 or Fe-nat, Pb-208 or Pb-nat) in order to demonstrate the feasibility and to test the setup and the method of analysis. We propose to continue with samples of interest, e.g. Al, V, Cr, Zr, Th, and U-238.

A few  $\times 10^{18}$  protons per sample in combined experiments with fission chambers is estimated as sufficient for the proposed experiments. It has to be emphasized that the expected count rates per detector and energy bin are rather low and a large number of protons is needed to obtain reasonable statistics.

---

<sup>12</sup> *Contributed by:* E Jericha, H Leeb, and A Pavlik (Atominsitut, Vienna University of Technology).

## Neutron scattering reactions<sup>13</sup>

Although the n\_TOF experimental activity aims at the determination of cross sections involving neutron-induced reactions essentially across the entire Periodic Table, the simplest of such cross sections,  $\sigma_{n+n}$ , eludes a direct measurement due to the unavailability of a free-neutron target. The low-energy,  $\ell = 0$ , cross section for the two nucleon interaction (NN) is usually expressed as a two parameter function involving the effective range  $r_{0NN}$  and scattering length  $a_{NN}$ , which have been accurately measured for the  $pp$  and  $np$  systems. On the other hand, the  $nn$  scattering length, which provides a very sensitive measure of the strength of the two-nucleon potential, and the  $nn$  effective range are known today with considerably poorer precision.

The proposed experiment at the CERN n\_TOF facility aims at determining the neutron-neutron interaction parameters through the interaction of the two neutrons in the final state of the reaction  ${}^2\text{H}(n,np)n$ . in the incident neutron energy range between 30 and 75 MeV. A cinematically “complete” experiment is envisaged, in which the momenta of one neutron and of the proton in the final state of the reaction will be measured in coincidence at specific detection angles with enhanced  $nn$  final-state interaction.

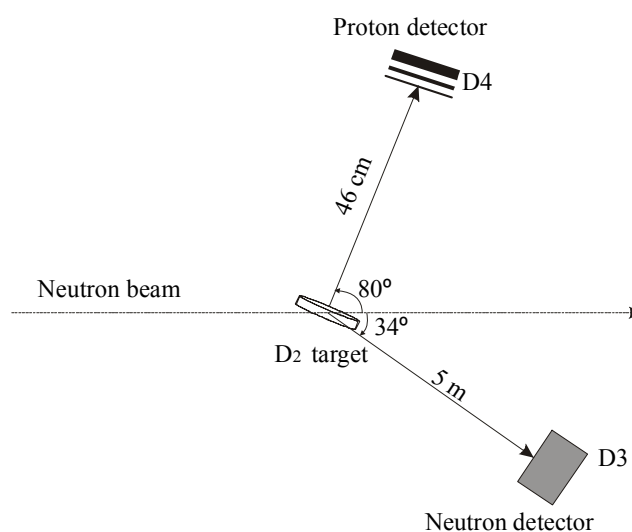


**Figure 25:** Schematic setup.

The experimental setup for the proposed study is shown schematically in Figure 25. The target will consist of deuterated polyethylene ( $\text{CD}_2$ ). Protons are recorded at a distance of about 50 cm from the target with a three-detector telescope, which will effect particle identification. One of the neutrons in the final state of the reaction will be detected by means of a plastic scintillator. The energy of the neutron

---

<sup>13</sup> Contributed by: PA Assimakopoulos (The University of Ioannina)

will be measured over a 5 m TOF path. Events obtained from the experimental setup in Figure 25 are best presented by a three-dimensional plot of population versus the two kinetic energies of the detected particles, where they are restricted on a kinematics locus determined by the overall energy and momentum conservation. For the particular setup of Figure 25 this locus is shown in Figure 26. For the direct break up of the deuteron, the population of events along the curve depicted in the figure will be governed by phase space. Events arising from the interaction of any pair of particles in the final state will appear as resonances along the locus.

Simulations of the corresponding spectra have been performed, taking into account the dimensions of the target and the detectors as well as the energy loss of the protons in the target. Figure 27 shows an example of such simulations where the resonance due to neutron-neutron interactions through the  $nn$  singlet state is depicted. The shape of the peak in this spectrum depends on the values of the parameters usually employed for the expression of the two-nucleon cross section, namely the scattering length and the effective range.

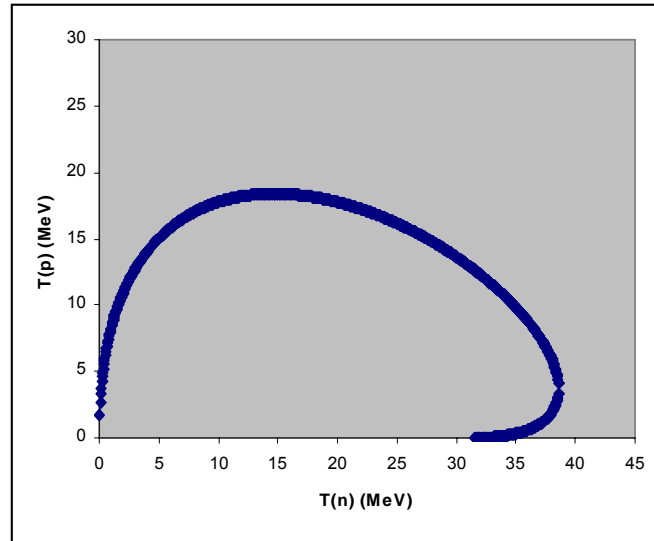
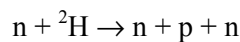


**Figure 26:** Kinematic locus for the reaction



at an incident energy of  $E_n = 50$  MeV. The neutron and proton are detected at angles  $\Theta_n = 35.5^\circ$ ,  $\Phi_n = 0^\circ$  and  $\Theta_p = 80^\circ$ ,  $\Phi_p = 180^\circ$ , respectively.

In the proposed experiment, spectra will be collected simultaneously in 2.5 MeV wide bins of incident neutron energy over a running time of one month, requiring a total of  $2 \cdot 10^{18}$  protons.

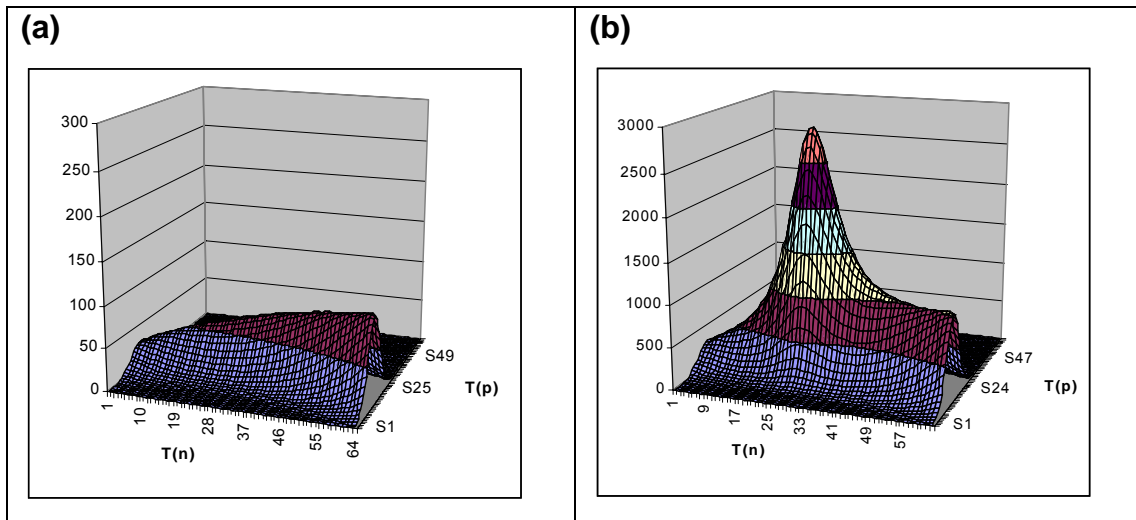


**Figure 27:** Simulated spectra around the  $nn$  singlet interaction resonance. **(a)** Phase space from the direct three-body break-up. **(b)** Total spectrum, including  $np$  and  $nn$  final state interactions.

## MEASUREMENTS RELATED TO DETECTOR DEVELOPMENTS

### Gas detectors<sup>14</sup>

While photons or charged particles interact primarily with the atomic electrons, producing ionization or atomic excitation, neutral particles like neutrons or neutrinos (or, more exotically, weakly interacting massive particles –WIMPs– candidate particles for dark matter) may interact directly with nuclei. The resulting nuclear recoil, at its turn, produces a short and intense track of ionization in the detector medium. The amount of ionization (ionization yield) produced by a nucleus recoiling with energy  $E$ , however, is less than the one produced by an electron of the same energy, the ratio, usually called *quenching factor*, being slightly dependent on the recoiling energy and, of course, on the nature of the medium.

The precise knowledge of the quenching factor is essential for experiments looking for low energy particle interactions when they are detected through the resulting nuclear recoil ionization. Examples of such experiments are those aiming at the detection of the coherent neutrino-nucleus interaction (predicted by the Standard Model but not yet experimentally observed), or those looking for hypothetical Dark Matter WIMPs. While usually solid (or liquid) state detectors are envisioned for those experiments (because of the large target masses usually needed to detect such low counting rates), a new version of gaseous detector, a spherical Time Projection Chamber (TPC), has been recently realized to be a most interesting option for the detection of the neutrino-nucleus interaction [27]. Although being a gaseous target, a spherical TPC can easily achieve large instrumented masses, while potentially keeping a very low energy threshold ( $\sim 100$  eV or even lower). Indeed, neutrinos interacting with nuclei produce nuclear recoils of extremely low energy (sub-keV or few keV range) and are out of reach of usual solid state detectors which do not offer those low thresholds for the large detector masses needed. The spherical TPC thus opens the way for the measurement of the neutrino-nucleus coherent scattering which, at its turn, will provide the way to study low energy physics in reactors and spallation sources or to detect neutrinos coming from supernovas.

The quenching factor in gases, which has not been thoroughly studied, especially at so low energies, remains one important question to be addressed for the preparation of a neutrino-nucleus experiment with a spherical gaseous TPC. In addition, gaseous detectors will play a very important role in next generation WIMP Dark Matter searches, because gas is the only medium in which one could aim at measuring the nuclear recoil direction, opening the way for a truly unmistakable WIMP signature. Progress is being done continuously, but certainly nuclear recoil directionality is still an experimental challenge. MICROMEGAS technology is very promising for that goal. The body of data obtained in a facility like n\_TOF would be extremely interesting to explore to which extent the imaging of nuclear recoil tracks is feasible, down to which energy and with which precision.

---

<sup>14</sup> *Contributed by:* IG Irastorza, S Andriamonje (CEA, Saclay), and I Savvidis (University of Thessaloniki)

Here we propose a series of measurements, using the n\_TOF beam, and a MICROMEGAS detector with 2 main goals. First the determination of the quenching factor down to very low energies (few keV) for several noble gases: He, Ne, Ar (and possible Xe). Second, the measurement of the nuclear recoil track with a MICROMEGAS fine readout.

At the moment 3 different approaches are considered. The final experimental set-up will depend on the results of ongoing studies and the availability of resources to carry on the necessary development toward the more complex options 2 and 3.

1. As a first simpler approach, a small MICROMEGAS detector, of already tested design (like the one, for instance, of [28]) would be placed in front of the n\_TOF beam, to measure the signals produced by the nuclear recoils. The time-of-flight measurement allows to single out the recoil spectra for each independent incident energy. The quenching factor is obtained by comparing the expected spectra (of recoiling energies) with the measured ones.
2. In this second arrangement, the MICROMEGAS detector is surrounded by several neutron detectors, located at distances of about 1 m, at several angles off the main neutron beam. The coincidence between one of these and the MICROMEGAS provides events for which the recoil energy is known (it is determined from the incident neutron energy and the angle). With this method the quenching factor is determined event-by-event and does not rely on the calculation of the expected recoiling spectra. On the other hand, this approach reduces the useful event rate by the fraction of solid angle covered by the neutron detectors. Ways to compensate this reduction may be needed to be pursued, like the use of larger MICROMEGAS detector or un-collimated n\_TOF beam.
3. The third approach is specifically addressed to the precise measurement of the nuclear recoil track. To this end, a fine 2D readout MICROMEGAS would be needed, with an upgraded electronics where the relative time of every pixel/strip would be recorded. A development is underway to study the feasibility of using the Medipix CMOS pixel array [29] (with pixel sizes of  $50 \times 50 \mu\text{m}^2$ ) together with MICROMEGAS in the present set-up.

We must stress that the proposed measurement can be performed in parasitic mode, due to the negligible effect done on the neutron beam by the interposition of the MICROMEGAS detector. The detector will be built with two thin windows (for the entrance and exit of the neutron beam), that together with the detector gas will be the only matter facing the neutron beam.

## Neutron cross-section measurements of relevance for Radiation Dosimetry, Radiation Protection and Radiation Transport<sup>15</sup>

The need for cross sections of neutron induced reactions in the energy range from a few tens of MeV up to the few hundreds of MeV has been pinpointed by several authors. In addition to data for innovative reactor concepts, measurements

---

<sup>15</sup> *Contributed by:* P Vaz (ITN, Lisbon), S Andriamonje (CEA, Saclay), and I Savvidis (University of Thessaloniki)

are requested in the field of neutron dosimetry and radiation protection as well as for medical applications in neutron and proton therapy. In these areas, quantities such as kerma factors in the tens of MeV range and cross sections for biologically relevant constituents of tissue and bones, i.e. for isotopes of hydrogen, carbon, nitrogen, oxygen, potassium, calcium, and phosphorus, and of mixed materials such as A-150 tissue equivalent plastic and ICRU-muscle have to be determined.

The interaction of neutrons in matter proceeds in two steps, the transfer of neutron kinetic energy to charged particles, and the deposition of that energy as the charged particles come to rest. Kerma and absorbed dose describe these processes, respectively, and are used to model the response of systems to neutron irradiation. Reliable neutron cross-section data to perform radiation transport calculations in the range above 20 MeV and to benchmark and validate predictions from physics models in this range are of paramount importance for these applications. In this respect charged particle yields from (n,x) reactions is of particular importance for the determination of kerma factors and for computing the absorbed dose.

Considering the excellent energy resolution and neutron beam characteristics in the MeV region make the n\_TOF facility perfectly suited for the measurements on biologically relevant nuclides and materials of interest for dosimetry and radiological protection studies.

For these measurements the spectral fluences of the n\_TOF spectrometer in the tens of MeV range should be verified by different detectors and techniques. The detectors specific to the proposed (n,x) measurements would be low-pressure proportional counters. The samples and phantoms are including the isotopes of H, C, N, O, K, Ca, and P as well as A-150 tissue equivalent plastic and an ICRU-sphere.

The neutron dose from the scattering neutrons around the n\_TOF beam, in the detectors area and in the working (monitors) area can be measured with several neutron detectors:

#### *The CR-39 neutron dosimeter*

CR-39 is a plastic passive nuclear track detector, which is insensitive to gamma rays, with a good sensitivity to protons and to heavy ions. The charged particles incoming in the detector produce a permanent track, which after a chemical etching becomes visible under an optical microscope. CR-39 neutron dosimeter has been calibrated in a neutron energy range from thermal up to 50 MeV [30][31]. The dosimeter consists of a CR-39 foil with two converters,  $^{10}\text{B}$  for (n, $\alpha$ ) reactions and 2 mm thick polyethylene for proton recoils. It is also in contact with a polyethylene plate with 1 cm thickness.

#### *TLD dosimeter*

TLD dosimetry in mixed Neutron and gamma radiation fields around the n\_TOF beam can be done using pairs of  $^6\text{LiF:Mg,Ti}$  -  $^7\text{LiF:Mg,Ti}$  dosimeters. Because of the very high cross section of  $^6\text{LiF}$  for thermal neutrons (945 barns compared with the 0.033 barns for  $^7\text{LiF}$ ), it has the highest thermal neutron sensitivity of any phosphor. In a mixed field  $^6\text{LiF}$  measures both thermal neutrons and gamma doses, whereas  $^7\text{LiF}$  measures only gamma dose. Since both dosimeters have the same sensitivity to gamma radiation, the thermal neutron dose is estimated

by subtraction of the gamma component measured by  ${}^7\text{LiF}$  from  ${}^6\text{LiF}$ . By using cadmium covers of appropriate thickness, dose contribution from higher-energy neutrons can be evaluated.

Count rate estimates appear difficult at present and have to be quantified in test experiments.



## REFERENCES

- [1] M Benedikt, *Will there be enough protons for physics in 2006-2010?* Presented at the Workshop *PS/SPS Days*, CERN, January 13-14 (2005). Slides available from the InDICO site: <http://indico.cern.ch/>
- [2] M Busso, R Gallino, and GJ Wasserburg, *Ann. Rev. Astron. Astrophys.* **37** 239 (1999).
- [3] F. Käppeler, *Prog. Part. Nucl. Phys.* **43** 419 (1999).
- [4] C. Sneden et al., *Ap. J.* **591** 936 (2003).
- [5] CM Raiteri, R Gallino, M Busso, D Neuberger, and F Käppeler, *Ap. J.* **419** **207** (1993).
- [6] T Rauscher, A Heger, RD Hoffman, and SE Woosley, *Ap. J.* **576** 323 (2002).
- [7] M Pignatari and R Gallino, *n\_BANT Workshop*, CERN, March 22-23, (2005).
- [8] K Takahashi and K Yokoi, *Atomic Data Nucl. Data Tables* **36** 375 (1987).
- [9] U Abondanno *et al.* (The n\_TOF Collaboration), *Phys. Rev. Lett.* **93** 161103 (2004).
- [10] G Aerts, *et al.*, (The n\_TOF collaboration), in *Nuclear Data for Science and Technology*, edited by RC Haight and MB Chadwick, in press (2005).
- [11] U Abbondanno *et al.* (The n\_TOF Collaboration), *Measurement of the neutron capture cross sections of  $^{233}\text{U}$ ,  $^{237}\text{Np}$ ,  $^{240,242}\text{Pu}$ ,  $^{241,243}\text{Am}$  and  $^{245}\text{Cm}$  with a Total Absorption Calorimeter at n\_TOF.* CERN INTC-2003-036, INTC-P-182, (2003).
- [12] D Cano-Ott *et al.* (The n\_TOF Collaboration), *Measurements at n\_TOF of the Neutron Capture Cross Section of Minor Actinides relevant to the Nuclear Waste Transmutation:  $^{237}\text{Np}$ ,  $^{240}\text{Pu}$  and  $^{243}\text{Am}$ .* Proceedings of the International Conference on Nuclear Data for Science and Technology, Santa Fe, September 2004, in press (2005).
- [13] C Rubbia *et al.*, *Conceptual design of a fast Neutron Operated High Power Energy Amplifier*, CERN/AT/95-44(ET); C Rubbia *et al.*, *Nuclear Waste Burner (NWB) – an ADS Industrial Prototype for Minor Actinides Elimination*, n\_TOF Winter School, Centre de Physique de Les Houches, February 2003.
- [14] E Gonzalez *et al.*, *Applied physics measurements at the n\_TOF facility.* Astrophysics, Symmetries, and Applied Physics at Spallation Neutron Sources, ASAP 2002. World Scientific. ISBN 981-238-249-6 (2002).
- [15] J Blons *et al.*, *Phys. Rev. Lett.* **35** 1749 (1975).
- [16] GA Tutin *et al.*, *Nucl. Instr. Meth. A* **457** 646 (2001).
- [17] W Lang *et al.*, *Nucl. Phys. A* **345** 34 (1980); H.J. Specht, *Phys. Scripta* **10A** 21 (1974); M.G. Itkis *et al.*, *Sov. J. Part. Nucl.* **19** 301 (1988).
- [18] K-H Schmidt *et al.*, *Nucl. Phys. A* **665** 221 (2000).

- [19] C Budtz-Joergensen *et al.*, Nucl. Instr. Meth. A **258** 209 (1987).
- [20] J Hamsch, private communication (2005).
- [21] P Mohr,  *$\alpha$ -nucleus potentials for the neutron-deficient  $p$  nuclei*, Phys Rev. **C62**, 045802 (2000).
- [22] YuP Popov *et al.*, *Investigation of  $\alpha$ -decay of  $^{148}\text{Sm}$  resonance states*, Nucl. Phys. A **188** 212 (1972).
- [23] PE Koehler, Yu M Gledenov, T Rausher, and C Fröhlich, *Resonance analysis of  $^{147}\text{Sm}(n, \alpha)$  cross sections: Comparison to statistical model calculations and indications of non-statistical effects*. Phys. Rev. C **69** 015803 (2004).
- [24] Yu M Gledenov, PE Koehler, J Andrzejewski, KH Guber, and T Rauscher,  *$^{147}\text{Sm}(n, \alpha)$  cross section measurements from 3 eV to 500 keV: Implications for explosive nucleosynthesis reaction rates*, Phys. Rev. C **62** R042801 (2000).
- [25] PE Koehler, *Comparison of white neutron sources for nuclear astrophysics experiments using very small samples*, Nucl. Instr. Meth. A **460** 352 (2001).
- [26] Y Giomataris, Nucl. Instr. Meth. A **419** 239 (1998); S Andriamonje *et al.*, Nucl. Instr. Meth. A **481** 120 (2002); Y Giomataris *et al.*, Nucl. Instr. Meth. A **379** 29 (1996).
- [27] I Giomataris *et al.*, talk given at 9th Topical Seminar on Innovative Particle and Radiation Detectors, Siena, May 2004. To be published in the proceedings (2005). See also: hepex/0502033 (2005); I Giomataris, *et al.*, talk given at Int. Workshop on Identification of Dark Matter (IDM2004), Edinburgh, September 2004. To be published in the proceedings (2005); IG Irastorza *et al.*, talk given at Int. Workshop on Low Radioactivity Techniques, Sudbury, Canada, December 2004. To be published in the proceedings.
- [28] S Andriamonje *et al.*, Nucl. Instr. Meth. A **518** 252 (2004).
- [29] P Colas *et al.*, Nucl. Instr. Meth. A **535** 536 (2004).
- [30] E Savvidis *et al.*, Nucl. Instr. Meth. B **94** 325 (1994).
- [31] E Savvidis and M. Zamani, Radiat. Prot. Dosim. **70** 83 (1997).